Title

Database Creation, Visualization, and Statistical Learning for Polymer Li
+
-Electrolyte Design

Journal

Chemistry of Materials, 33(13)

ISSN

0897-4756 1520-5002

Authors

Schauser, Nicole S
Kliegle, Gabrielle A
Cooke, Piper
et al.

Publication Date

2021-06-21

DOI

10.1021/acs.chemmater.0c04767

Peer reviewed

Database Creation, Visualization, and Statistical Learning for Polymer Li^+ Electrolyte Design

Nicole S. Schauser,[†,‡,¶] Gabrielle A. Kliegle,[§] Piper Cooke,[§]

Rachel A. Segalman,[*,‡,†,‖] and Ram Seshadri[*,‡,†,§]

†*Materials Department*

University of California, Santa Barbara, California 93106, United States

‡*Materials Research Laboratory*

University of California, Santa Barbara, California 93106, United States

¶*Mitsubishi Chemical Center for Advanced Materials*

University of California, Santa Barbara, California 93106, United States

§*Department of Chemistry and Biochemistry*

University of California, Santa Barbara, California 93106, United States

‖*Department of Chemical Engineering*

University of California, Santa Barbara, California 93106, United States

E-mail: segalman@ucsb.edu; seshadri@mrl.ucsb.edu

Abstract

Visualization and statistical regression of compiled datasets is emerging as a powerful tool in understanding and screening the design space of materials properties, rapidly providing insights that would not be readily gained from studies of individual systems. We describe here, the curation and analysis of a database of polymer Li^+ electrolyte conductivity performance, manually extracted from the published literature. We focus on solid, dry polymer electrolytes without additives. Data was extracted from 65 publications, resulting in 655 unique polymer–anion–salt concentration entries and 5225 individual conductivity data points to create an interactive database: `PEDatamine.org`. Visualization of the collective dataset suggested that individual features, other than the activation energy, are poor predictors of conductivity performance across the wide range of polymer chemistries, Li salts, and salt concentrations examined. The Meyer-Neldel rule suggesting a correlation between the conductivity prefactor and activation energy is shown to hold universally for both Arrhenius and Vogel-Fulcher-Tammann representations. Statistical regression techniques were employed to extract the most important features relevant in determining Li^+-ion conductivity. These include polymer molecular weight, glass transition temperature, existence of electronegative heteroatoms in the monomer, and anion size. However, experimental features can be omitted from the regression model without impacting predictive performance, reinforcing the importance of monomer electronegativity, hydrogen bonding, and anion molecular bulk.

Introduction

A significant body of work over the past half-century has focused on the improvement of ionic conductivity of solid polymer electrolytes.[1–3] Solid polymer electrolytes are potentially safer, more mechanically robust, and more chemically stable than the organic liquid electrolytes currently employed in electrochemical energy storage devices. However, their conductivity performance is at least an order of magnitude below the required target for practical applications.[4] While several reviews have been published on various classes of polymer electrolytes, there has not so far been a large-scale analysis of published data, to extract fundamental understanding and design principles.

There exist in the literature, several studies of specific polymer electrolyte families that attempt to develop design principles, but it is unclear whether what is learned is applicable to a broader range of polymer chemistries. For example, while the importance of low polymer T_g and intermediate ligand density has been studied in optimizing ionic conductivity in imidazole side-chain grafted polysiloxanes,[5] other studies have compared polymers with low and high T_g and shown that the T_g is less important than other chemical features of the polymer.[6,7] Thus, while detailed studies across a single polymer families are important for determining design rules associated with the specific polymer chemistry, salt identity, processing conditions, *etc.*, it is possible that a study across a broader range of polymer electrolyte materials could reveal design rules or insights not otherwise foreseen.

Data visualization and machine learning have recently gained prominence in materials science for improving understanding and predicting new compounds in a variety of applications ranging from thermoelectrics,[8–10] to inorganic battery materials,[11–15] to electronic materials,[16–18] to other functional materials.[19–21] Polymers have also been the recent subject of recent data-driven discovery, including the prediction of polymer glass transition temperature, T_g,[22–24] exploration of new polymer electrolytes,[25–27] and prediction of gas diffusion in membranes.[28]

Data visualization on its own can be immensely powerful, both to extract trends in ag-

gregate data that may have been missed in smaller studies, as well as to highlight important gaps in published literature that should be corrected.[29–31] The addition of machine or statistical learning techniques can aid in situations where more complicated relationships exist between descriptors and the quantity of interest; in such cases simpler visualizations do not readily show trends.[32]

While data mining, visualization and machine learning are powerful tools in their ability to help advance materials discovery and optimization, they also have limitations in their applicability. The first is that data extraction from the published literature is currently a labor-intensive manual process for many materials studies, as data exist usually within figures in publications, rather than in pre-existing databases. While natural language processing will no doubt aid in future efforts, current studies generally rely on manual extraction and require domain knowledge to parse important features from each study. Data quality can also restrict the impact of data mining efforts; many studies do not report all relevant processing parameters, materials characteristics, and measurement conditions.[33] The limited size that can be manually extracted of many of the datasets also creates questions of data reproducibility, as it is more challenging to spot clear outliers in sparse datasets. A small number of entries and a large number of possible descriptors can also significantly impede machine or statistical learning techniques, which can suffer from severe over-fitting either due to the small size of the dataset or the lack of relevant descriptors reported in the original studies.

In spite of these limitations, data visualization and simple statistical analysis can still provide insight into the state and future direction of solid polymer electrolytes. We therefore set out to curate a database of polymer electrolytes for the visualization and statistical learning of features that may be important predictors of ionic conductivity performance. The work-flow followed in this study is shown in Figure 1. This study is limited to solid polymer Li^+-electrolytes without solvent or other additives, and includes a database compiled from 65 publications with 655 unique polymer-anion-salt concentration entries and

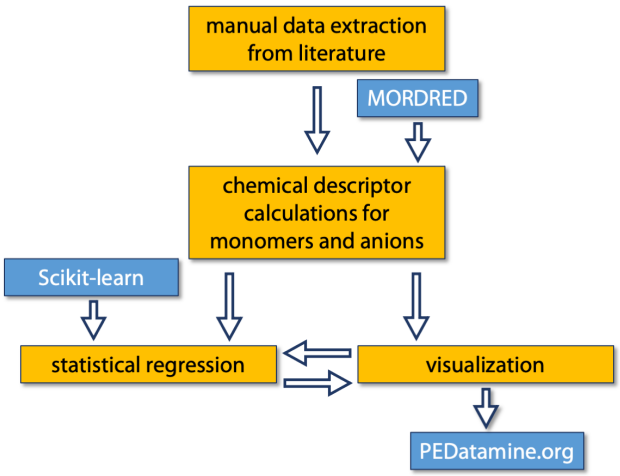

Figure 1: The visualization study included manual extraction of data from relevant literature, calculation of relevant chemical descriptors, manual visualization using Python and a custom webpage, and statistical regression implemented using the Python Scikit-Learn library.

5225 conductivity data points. While the dataset includes a mixture of crystalline and amorphous systems, with a wide range of polymer chemistries and some varying polymer architectures (*i.e.* linear versus branched), it does not cover block copolymers, electrolytes with additives, or single-ion conductors. The scope is thus limited to lithium-based polymer + salt systems.

We find that no single parameter, other than the measured activation energy, adequately correlates with ionic conductivity performance over the entire range of polymers compiled in this study. While some correlations exist for specific chemical identities, such as T_g in a range of carbonate-ether copolymers, most polymer families do not actually show strong trends with any of the features previously predicted to influence conductivity behavior. Meanwhile, we confirm the universality of the previously-reported Meyer-Neldel rule, or compensation effect, for the broad range of polymer electrolytes examined in this study.[34–36] The Meyer-Neldel rule observes a linear relationship between activation energy and the logarithm of the pre-exponential factor and has been observed for many activated hopping processes in materials science. Importantly, we show that a strong Meyer-Neldel

correlation does not translate to the ability to predict conductivity from activation energy alone, since small errors in activation energy have an exponential effect on conductivity. Statistical regression techniques reveal that the most important features for the prediction of conductivity are polymer molecular weight (MW), glass transition temperature (T_g), existence of electronegative heteroatoms in a monomer, and anion size. However, these features are not determinant, since the removal of experimental features (including molecular weight and T_g) still allows for adequate performance prediction, emphasizing the ability to obtain adequate performance predictions without the need for experimental parameter inputs. Furthermore, efforts to limit data leakage in statistical learning by grouping the entries by polymer and anion identity results in poor model performance, and illustrates the difficulty in using such models for the prediction of previously unexplored polymer electrolytes. This underscores the general interdependence of features and complexity of polymer electrolyte conductivity prediction.

Methods

The data used for this work was manually extracted from the literature.[5–7,37–98] Publications were selected from two major reviews,[1,2] as well as from additional literature searches. Data was restricted to solid polymer electrolytes without additives, where the reported conductivity and characterization did not immediately look suspect. Random copolymers were included, but block copolymers were excluded due to the existence of additional factors complicating conductivity response, such as the possibility for self-assembly into more complex morphologies which affects conductivity on a volumetric basis. The literature provides a wide range of conductivity performance, but is likely skewed towards specific materials classes (*e.g.* many more studies on ether-based polymers than other polymers). Attempts were made to keep the distribution of polymer chemistries as even as possible, though over half of all polymers examined here incorporated ether functional

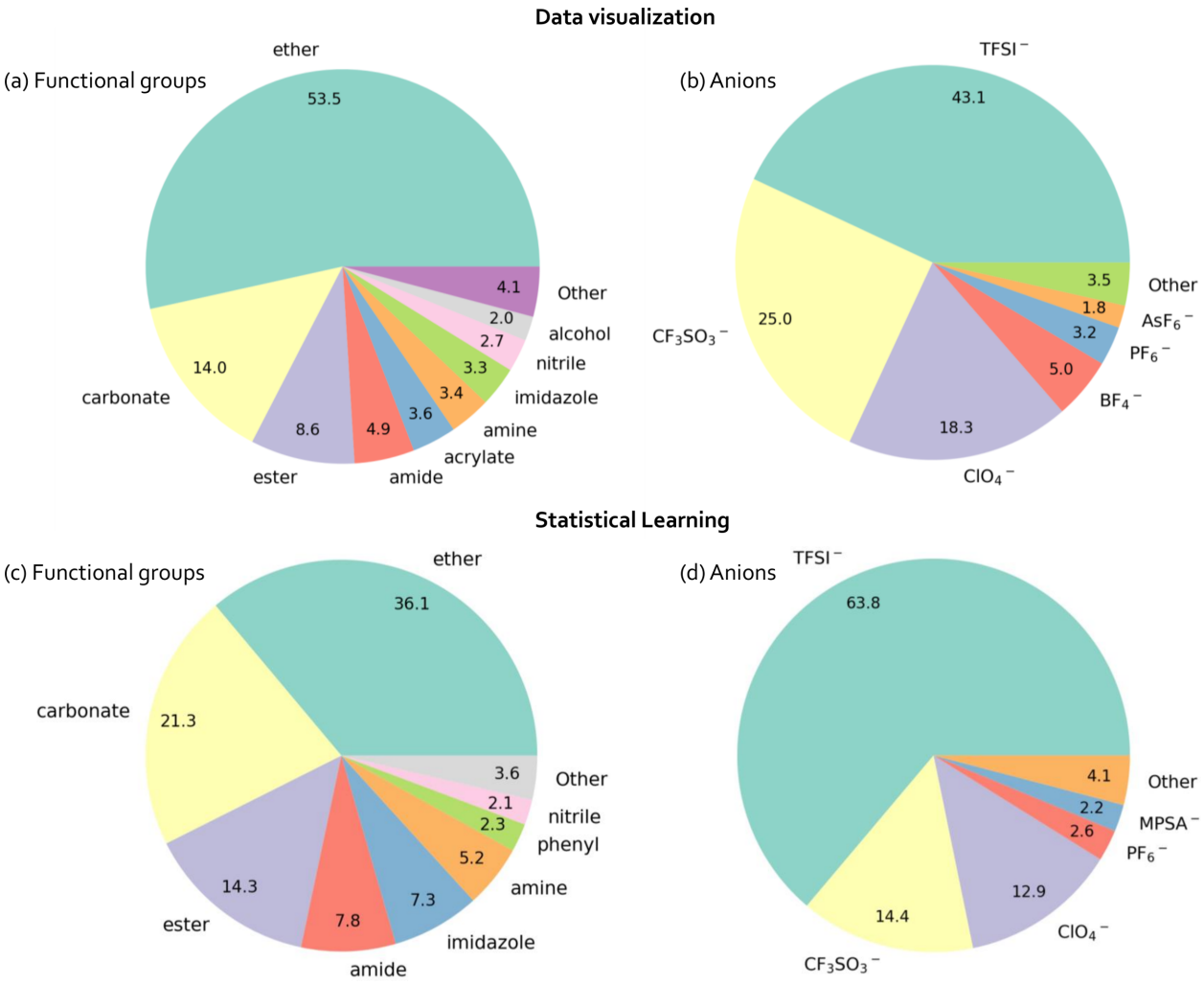

Figure 2: Distribution of polymeric functional groups and anions in entries included for visualization data and statistical learning data. (a) Functional groups extracted in this study include ethers, carbonates, esters, amides, and others. (b) Many Li-based salts were studied, with the highest prevalence for $TFSI^-$ and $CF_3SO_3^-$. (c) Entries extracted for statistical regression shift the distribution of functional groups to lower ether contents. (d) Upon dataset trimming for statistical regression, the prevalence of $TFSI^-$ anions increased.

groups; the fraction of entries for the various functional groups and Li salt identities is shown in Figure 2.

Conductivity values and T_g values published in figures were extracted using WebPlotDigitizer.[99] Additional descriptors, such as polymer molecular weight, processing conditions and salt concentrations were extracted from the text, tables or figures. For procedures with multiple drying or processing steps, the most rigorous (highest vacuum or temperature) processing step was included. When no drying vacuum was mentioned, it was assumed that no vacuum was used. For electrolyte concentration series where some T_g values were provided but others were omitted, the T_g versus salt concentration data was interpolated to extract approximate T_g values for intermediate salt concentrations. Electrolyte conductivity as a function of temperature data was fit to Arrhenius (Equation 1) and Vogel-Fulcher-Tammann (VFT) conductivity functions. For VFT fitting, two methods were used. The first kept T_0 as a fit parameter (Equation 2), while the second set $T_0 = T_g - 50$, when T_g was provided (Equation 3).

$$\sigma = A \exp\left(\frac{-E_a}{k_B T}\right) \tag{1}$$

$$\sigma = A T^{-\frac{1}{2}} \exp\left(\frac{-B}{T - T_0}\right) \tag{2}$$

$$\sigma = A T^{-\frac{1}{2}} \exp\left(\frac{-B}{T - T_g + 50}\right) \tag{3}$$

After data retrieval, Python scripts were developed to clean and organize the data for visualization and statistical regression. An approximate polymer molecular weight was extracted as an additional column which was either the number-averaged molecular weight (M_n), when provided, or the weight-averaged molecular weight when M_n was not provided; if no molecular weight was provided, the column was left blank. The solvent used for the processing steps was listed by its boiling point. In addition to the features extracted

from the publications, chemical descriptors were calculated based on the polymer and anion identity. The MORDRED library[100] was used to calculate polymer and anion descriptors after manual input of the monomer and anion structure in SMILES format. BigSMILES notation has been suggested for use with polymer systems,[101] but is not yet compatible with Python libraries such as MORDRED and was therefore not used in this study. For some monomer structures, manual correction of number of hydrogen bond donors and acid groups was necessary due to the implicit addition of hydrogens to dangling bonds (e.g. C-O becomes C-OH). For the PF_6^- anion, many MORDRED ExtendedTopochemical Atom parameters were not calculable because the bonding count to the central atom is greater than 4; for these values, the average of that column for all the other anions was substituted. Only a subset of the full list of chemical descriptors were calculated using MORDRED; those parameters that are expected to most influence physical and electronic structure were included. A list of the descriptors manually collected and used for visualization can be found in Table 1; the subclasses of descriptors calculated using the MORDRED library are Polarizability, HydrogenBond, RotatableBond, VdwVolumeABC, Weight, AcidBase, AtomCount, ExtendedTopochemicalAtom, and KappaShapeIndex.

Table 1: List of manually collected descriptors.

Polymer characteristics	Processing/Performance characteristics	Salt characteristics
Polymer functional groups	Conductivities at 0 °C to 125 °C	Anion identity
Polymer	Li^+ t_+	Salt concentration
SMILES comonomer 1	VFT/Arrhenius prefactors	(Li:functional group)
SMILES comonomer 2	VFT/Arrhenius activation energies	
Comonomer percentage	Li^+ diffusion coefficient	
T_g	Viscosity	
T_g w/out salt	Storage modulus	
Is crystalline?	Young's modulus	
T_m	Solvent used	
M_n or M_w	Drying temp	
Đ	Drying vacuum	
Chain architecture		

The data was then visualized using MatPlotLib[102] and Seaborn in Python, as well as

using Plotly and Dash as a webpage.[103] The webpage includes pages for visualization of data trends, conductivity plotting, a view of the correlation matrix of the descriptors used in the statistical regression portion of the study, and links to the curated dataset as well as the original paper DOIs. This webpage is accessible to the larger community for additional exploration of dataset trends.

After visualization, the dataset was pruned further for statistical regression analysis. Ordinal categorical features such as crystallinity and vacuum strength used for the drying procedure were converted into sequential numbers, while chain architecture was converted to arrays using one-hot encoding. When no explicit electrolyte drying temperature was provided, 25 °C was assumed; when no drying time was provided, a nominal time of 8 h was entered for the dataset used for statistical learning.

Many features were dropped from the initial data set to optimize for a maximum number of entries while still including the most relevant features expected to contribute to conductivity performance. This feature selection was necessary since many entries had missing values for many features. Dataset manipulation and regression techniques were implemented in Python using the Scikit-Learn library.[104] After removing all entries with missing values, the dataset was split into a training and a test set, with 20% of the entries (55 entries) in the test set. Highly correlated features (with a correlation > 0.99) were dropped from the features list, after which recursive feature elimination on the training data using a random forest algorithm and 5-fold cross-validation further reduced the number of features to an optimized amount. The final dataset used for statistical regression had 271 entries and 36 features. The target property for prediction was chosen as the base-10 logarithm of the total ionic conductivity at 60 °C, as this was the temperature at which the most entries recorded conductivity (389 entries from the original 655, or 60% reporting). The reduction from 389 to 271 entries is due to other missing features such as T_g and approximate molecular weight.

We then used machine learning models implemented in Scikit-Learn to explore feature

importances in predicting conductivity performance. A pipeline was constructed for data manipulation and fitting – this includes standardizing then normalizing the data before fitting the data with the appropriate regression model. A simple dummy regressor was compared to ridge regression, random forest regression, gradient boosting regression and extra trees regression models. These models were chosen as they enable extraction of feature importances. Grid search and 5-fold cross-validation were used on the training data to optimize model hyper-parameters for each algorithm, taking care to set the random state for reproducible cross-validation splits for each algorithm. Mean squared error was used as the scoring criterion. The hyperparameters were tuned using grid search to select the best parameters for each algorithm.[104]

Once the hyperparameters were selected, the different algorithms were compared against each other, again using 5-fold cross-validation. Averaged mean squared error, averaged mean absolute error and averaged R^2 were all evaluated as scoring criteria. All algorithms were then re-trained on the entire training dataset and the top 10 most important features were compared between the models. The random forest algorithm performed best on the cross-validated training data in all metrics and is discussed herein, while the other models are discussed in the Supplementary Information. Lastly, the trained random forest model was evaluated on the test dataset.

In addition to a randomized dataset splitting into test, train and validation sets, grouped splitting was also attempted using Scikit-Learn's GroupShuffleSplit and GroupKFold. This splitting eliminates any data leakage between the train and validation or test sets for the groupings that were selected. Groupings were done by polymer type, as well as polymer+anion, which eliminates the possibility of that electrolyte combination occurring in both the training and validation/test datasets just at a different salt concentration or different processing conditions. Feature reduction using correlations and recursive feature elimination, pipeline construction, model hyperparameter tuning, and model fitting was repeated as before except with the additional constraint of using grouped splits for train-

test split and cross-validation. Performances were compared between models, but were too low to motivate further model exploration.

Results and Discussion

The goal of this study is to explore trends in conductivity performance over the vast array of published work on solid polymer electrolytes. Through a combination of data mining, visualization, and statistical regression techniques, we have attempted to extract the most important features and predictors of ionic conductivity in additive-free polymer electrolyte systems (Figure 1). We began by selecting publications containing solid polymer electrolyte conductivity data, with an attempt to explore the performance from a representative range of polymers/functional groups found in the literature. After manual data extraction, the dataset was cleaned using Python, and additional descriptors for polymer and anion identity were calculated using the MORDRED library.[100] The full dataset was used for manual and web-assisted visualization of trends, while a smaller cleaned data set with the removal of rows and columns containing empty values was used for subsequent statistical regression analysis.

In an effort to limit the data mining study to a data subset that is feasible for manual collection, the scope of this study includes polymer-salt electrolytes *without* additives such as plasticizers, ionic liquids or inorganic fillers. While a much broader set of studies on polymer electrolytes have been published since the discovery of the ion-conducting properties of poly(ethylene oxide) in the 1970s,[105] our approach explores fundamental ion transport mechanisms in polymers – once additives are mixed into the polymer electrolyte, ion transport mechanisms can alter substantially, reducing the ability to draw cohesive conclusions from a single subset of studies.

For this study, 655 polymer-anion-salt concentration samples ('entries') from 78 polymers and 65 publications were selected from reviews and primary literature for data ex-

traction and examination. Each entry contains conductivity data spanning multiple temperatures, resulting in 5225 total conductivity points. Trimming the dataset for statistical learning reduced these numbers to 271 entries from 50 polymers. Figure 2 shows the distribution of polymer classes and anions of the data examined in this study for data visualization (a,b) and statistical learning (c,d). Some polymers contained more than one functional group, either due to co-polymerization or because the monomer contained multiple functional groups – the visualizations here show the percentages for each functional group, such that polymers with multiple functional groups will contribute to each functional group percentage. For data visualization, functional groups listed in the 'Other' category include phosphazene (14 entries, 1.64%), phenyl (12 entries, 1.41%), sulfonyl (5 entries, 0.59%) and carbonyl (4 entries, 0.47%). The anions included in the 'Other' category include $MPSA^-$ (6 entries, 0.92%), $AlCl_4^-$ (6 entries, 0.92%), $N(SO_2C_2F_5)^-$ (4 entries, 0.61%), I^- (4 entries, 0.61%), SCN^- (2 entries, 0.31%) and FSI^- (1 entry, 0.15%).

Trimming the dataset for statistical learning led to an improvement in the distribution of functional groups, but weighted the anion choice heavily towards $TFSI^-$ (see Figure 2c,d). For statistical learning, functional groups listed in the 'Other' category include acrylates (6 entries, 1.56%), alcohols (4 entries, 1.04%), and carbonyls(4 entries, 1.04%). The anions listed in the 'Other' category include $N(SO_2C_2F_5)^-$ (4 entries, 1.48%), BF_4^- (4 entries, 1.48%), SCN^- (2 entries, 0.74%) and FSI^- (1 entry, 0.37%). While this imbalance may lead to difficulties in the prediction capability for statistical learning models, this is unavoidable due to the lack of complete literature data for many publications.

Data quality and completeness is a continuous concern in scientific research, and was an issue for many of the manuscripts examined for data extraction for this study. In both older and more recent literature, instances of missing processing parameters (polymer-salt mixing solvent, drying procedures, etc.), polymer properties (molecular weight, dispersity), and electrolyte properties (glass transition temperature, lithium transport number) were prevalent and limited the scope of the current study. This is a commonly-discussed

issue in materials data-mining and machine learning studies, where the ability to draw conclusions based on published data is hindered by the limited knowledge of the large number of factors that can affect material performance.[22,33] To balance data completeness and overall data quantity, all data was included for the manual visualization component of the study, while a subset of relevant features were selected for statistical learning. Further, the low overall quantity of data, relative to fields where statistical regression and machine learning have been traditionally applied, prevents easy visualization of outliers. In this work, an attempt was made to filter studies with questionable data quality (i.e. lack of reasonable drying conditions for polymers, suspect impedance spectroscopy curves, etc.), but more work should be done in carefully and systematically characterizing processing parameters for polymer electrolytes in order to validate and explore the conclusions presented here.

Data visualization

The large body of fundamental studies on polymer ion transport mechanisms suggests some key features that are likely to show predictive trends in ionic conductivity performance. These include the polymer electrolyte glass transition temperature (T_g),[106–108] conductivity activation energy,[109] anion size and electrostatic interaction with the Li^+,[110,111] polymer dielectric constant,[112–117] and salt concentration.[86,118,119]

Plotting some of these features against the electrolyte ionic conductivity at 60 °C reveals the danger in focusing on singular design metrics for universal performance improvements (Figure 3). While some features show reasonable correlation to the ionic conductivity (e.g. Arrhenius activation energy, E_a), all features still exhibit significant scatter in conductivity performance. That is, for a single value of T_g, E_a or other feature, the reported ionic conductivities still vary by multiple orders of magnitude. This underscores the difficulty of extracting a single feature or electrolyte descriptor that can be used to predict or explain conductivity performance.

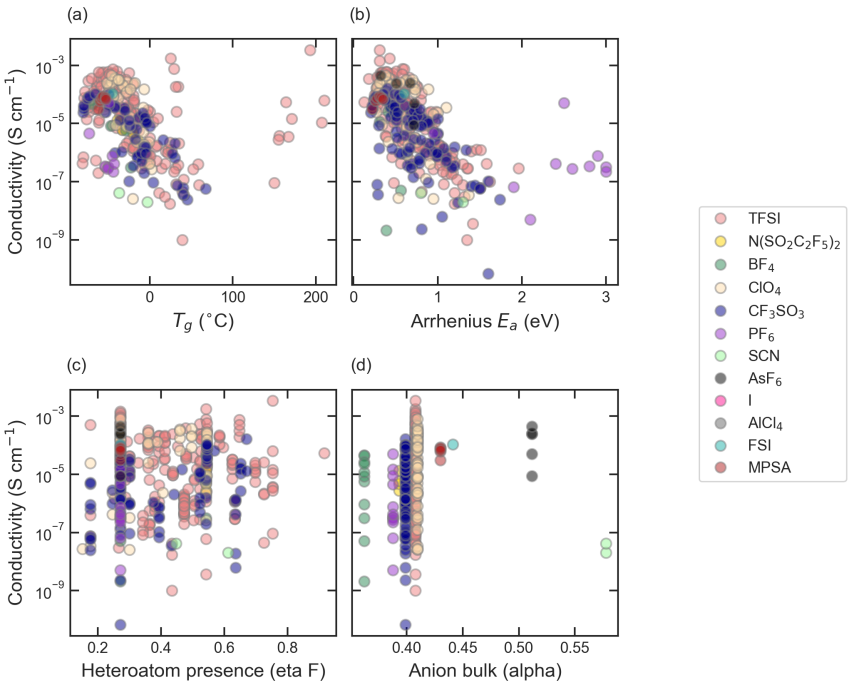

Figure 3: Scatter plots showing the lack of correlation between most features and the total ionic conductivity at 60 °C. Some correlation exists for T_g and activation energy (E_a).

A commonly discussed polymer characteristic that is expected to influence conductivity performance is polymer T_g.[5,106–109] From a fundamental perspective, the local polymer segmental relaxation/re-arrangement time rather than the bulk T_g is expected to govern ion mobility by affecting ion hopping rates through the rubbery polymer electrolyte.[109] This arises due to the complexation of Li^+ ions by solvation sites along the polymer chain, resulting in strongly correlated motion between the mobile ions and local polymer segments.[120] While anions are typically not directly solvated by the polymer chains, they are still dependent on segmental motion creating hopping pathways for anions through the polymer melt. Many studies use T_g as a proxy for more local dynamics due to the generally strong correlation between the polymer T_g and segmental relaxation dynamics. Individual studies on polymers ranging from polyethers[111] to sidechain-grafted imidazoles[5] have shown that a lower polymer T_g generally improves the ionic conductivity for rubbery polymer electrolytes. In the case of PEO, the effect of local segmental dynamics in determining

ionic conductivity has been directly determined using quasi-elastic neutron scattering.[106] On the basis of such individual studies, lowering polymer T_g is a common design strategy cited in the literature in the search for higher-performance polymer electrolytes.[1,3]

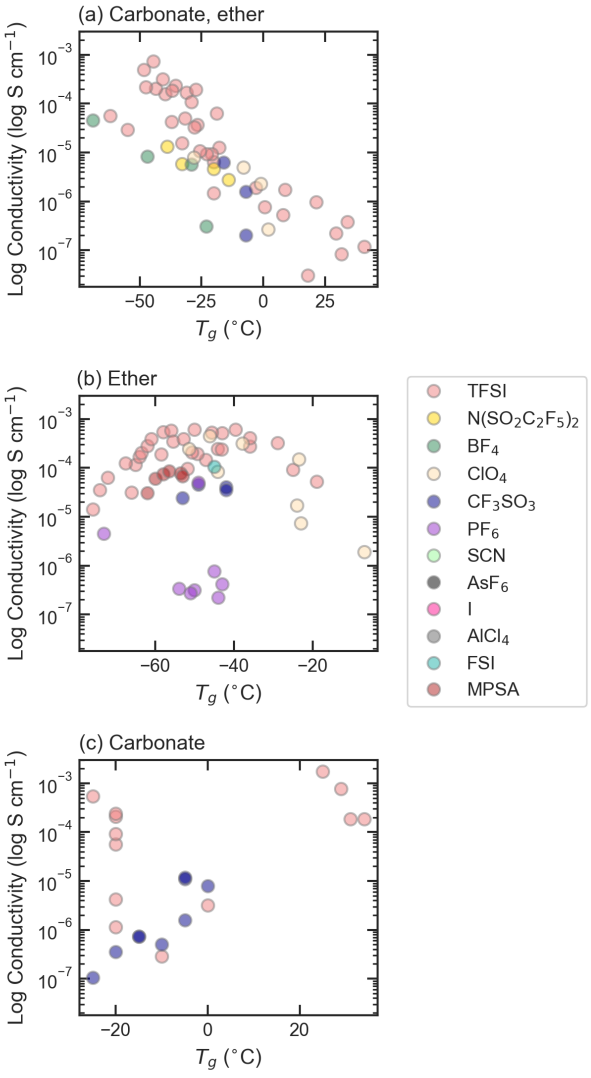

Figure 4: T_g is not a good predictor for ionic conductivity at 60 °C for all polymer classes; (a) while a lower T_g leads to higher conductivities for polymers with carbonate and ether functional groups, there is no trend for (b) pure polyethers, and a slightly positive trend for (c) pure polycarbonates.

As Figure 4 shows, the glass transition temperature is not the sole indicator of ionic conductivity performance in most polymer electrolyte classes. Copolymers based on car-

bonate and ether functional groups seem to show a clear trend with T_g, while the more general class of purely ether-based polymers shows no clear trend with T_g. Interestingly, polymers with only carbonate functional groups even seemed to show slight reversal of the expected conductivity trend with T_g, though the limited data for this family makes drawing broad conclusions challenging. However, the lack of a clear universal trend in conductivity with polymer T_g also underscores the difficulty in attempting to find proxies for fundamental parameters expected to control ionic conductivity.

While a correlation between ionic conductivity and segmental motion is fundamentally expected for many rubbery polymers, additional factors are likely affecting the universality of this T_g-conductivity relation. The ether and carbonate polymer families are more likely to be semi-crystalline, which might play a role in the importance and applicability of T_g as a metric. It is also possible that differences in processing parameters (e.g. solvent identity, drying time, measurement conditions) is affecting the reproducibility of trends seen in individual studies. This is especially likely for polymers such as polyethers which easily absorb water and whose processing parameters were not rigorously controlled in early studies.

Additionally, ion transport in some polymer electrolytes may follow mechanisms different from the proposed segmental dynamics-assisted ion motion. For example, polymer electrolytes with high T_gs and rigid backbones are expected to follow a more solid-like conductivity mechanism in which local re-arrangements are less important, and ions hop through pre-existing pathways in the rigid structure.[1,93,109,121] While such a mechanism is not expected for most polymers reported here, the possibility for conductivity mechanisms spanning these two extremes is also important to consider. Intermediate mechanisms of ion transport can be described by dynamic percolation theory,[122–125] in which both the ion hopping and segmental re-arrangement timescales are relevant to consider. In the first extreme, ion hopping is much faster than segmental re-arrangement, and a solid-like conduction mechanism is observed. The other extreme results in a liquid-like mechanism,

where segmental re-arrangements dominate the conduction behavior. The continuum between these two extremes suggests that perhaps both segmental re-arrangements – possibly explained by T_g – *and* ion hopping – governed by functional group identity, polymer structure, etc. – are important for conductivity performance, thus resulting in a greater-than-expected spread in conductivity *vs.* T_g data. Dynamic percolation theory is likely linked to related discussions suggesting that fragility of glass formation, rather than T_g be used as a proxy for ionic conductivity performance due to the strong decoupling between ion motion and T_g that can result.[66,121]

Anion identity has also been suggested to correlate with conductivity performance in individual polymer studies,[110,111] but does not provide a strong prediction of ionic conductivity in the aggregated data set (Figure 3d). Anion size and polarity affects salt dissociation within the polymer, the extent of polymer matrix plasticization, and anion hopping mobility. However, it is likely that anion effects are overwhelmed by a range of other factors that are known to affect ion mobility, such as polymer polarity, cation solvation ability, salt concentration, and ion aggregation. This underscores the realization that many features work in concert to influence ionic conductivity, resulting in sometimes limited information gained from a single descriptor.

A simple correlation between activation energy and Arrhenius (or VFT, see SI) prefactor exists for the entire range of polymers examined in this study (Figure 5a) and follows the form

$$ln(A) = mE_a + b \tag{4}$$

Known as the Meyer-Neldel rule, isokinetic relationship, or compensation effect,[34–36,126] this correlation is expected to be a very general result for all systems with large activation energy.[35] Indeed, it has been shown to hold for activated ion transport processes in a number of inorganic and organic materials, including poly(ethylene oxide) following Arrhenius temperature dependence,[126] and single-ion conducting polymers with VFT behavior.[34] A similar relationship holds for small gas molecule diffusion through both glassy or rubbery

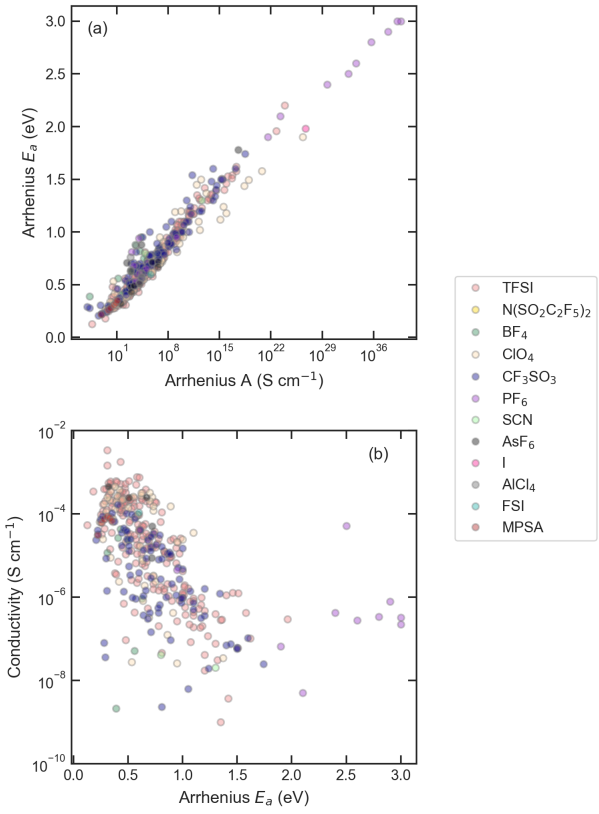

Figure 5: (a) Arrhenius activation energy correlates strongly with conductivity pre-factor, confirming the generality of the Meyer-Neldel rule. (b) Arrhenius activation energy correlates somewhat with ionic conductivity, though outliers and data spread exist.

polymer membranes.[127] In these materials, the slope, m, of the correlation was found to be independent of both gas and polymer type, while there was some change in correlation intercept, b, between rubbery and glassy polymers.

The microscopic understanding of this correlation has been described in terms of the connection between activated hopping energy (enthalpy) and the number of pathways that are available for hopping (entropy).[35,126] In gas diffusion, it was suggested that the similar slope of the natural logarithm of diffusion coefficients versus diffusion activation energy indicates diffusion mechanism to be invariant with gas identity or polymer identity within either rubbery or glassy polymers.[127] This universality also exists for both Arrhenius and VFT conductivity fits for the wide range of polymer functional groups, salt identities and salt concentrations of the lithium-conducting solid polymer electrolytes examined in this study, similarly suggesting that chemical environment (e.g. solvation functional group, anion identity, etc.), as well as differences in T_g or crystallinity do not appreciably affect the mechanism of ion transport through polymer electrolytes. Interestingly, this holds even for the small number of rigid or high T_g polymer systems included in this study, where the reported ionic conductivities occurs well below T_g.

Many interpretations of Arrhenius or VFT fitting of conductivity data attribute significance to both the resulting activation energy (energy barrier for ion transport) and the prefactor, which is most often used to compare relative mobile ion concentrations between samples. A standard derivation of the Arrhenius conductivity equation suggests the prefactor is a combination of both the number of mobile ions as well as a diffusion prefactor which depends on the vibrational attempt frequency and structural parameters. Since the correlation between activation energy and prefactor has been shown to hold for both diffusion equations as well as conductivity equations, it is likely that the correlation observed in the case of conductivity stems directly from the connection between diffusion prefactor and activation energy, rather than ion concentration. Thus, while it has previously been suggested that the strong correlation between these two parameters negates the pos-

sibility of optimizing for easy ion transport (low activation energy) and high mobile ion concentration simultaneously,[34] it is possible that instead this correlation only highlights the connection between activation energy and attempt frequency, rather than mobile ion content. The origins of the prefactor-activation energy correlation for the conductivity equation could be probed more directly using other techniques, such as solid-state NMR, that can quantify either mobile ion content or ion hopping attempt frequency.

While it is tempting to argue that the strong correlation between activation energy and prefactor should enable conductivity prediction from activation energy calculations, Figure 5b emphasizes that activation energy does not universally predict conductivity performance. Thus, the Meyer-Neldel correlation is somewhat deceptive in its utility, since a given activation energy still shows a large spread in conductivity performance. This is likely explained by the exponential nature of the activation energy, resulting in significant changes in ionic conductivity given only small fluctuations in E_a.

The visualization results discussed above emphasize the difficulty in determining universal predictors for conductivity performance in additive-free solid polymer electrolytes. While we have discussed a few of the likely important features in the text above, we emphasize that additional features describing anion and polymer properties (including un-characterized or un-reported features such as ion aggregation structure) are likely to play a role in determining conductivity performance. For those descriptors that are documented, we now turn towards statistical regression techniques to extract more complex relationships between the various features and the total conductivity performance.

Statistical regression analysis

Statistical regression and machine learning present appealing opportunities to uncover trends and connections in datasets that are not immediately apparent to humans. This is generally the case when many of the expected and possibly important features do not seem to strongly correlate with the property of interest (*e.g.* conductivity), as was discussed

above. A general trade-off exists between model prediction capability and interpretability; simple models are easily interpretable but often do not achieve the same prediction capability compared to more complex models.[32] Since the goal of the statistical regression implementation in this instance is to extract important descriptors, relatively simple regression models were chosen.

Many features that were included in the manual visualization portion of the study were dropped for the statistical regression. Most were dropped due to lack of data for many of the polymer entries. However, we also chose to drop the activation energy and prefactor terms from Arrhenius or VFT fits. Due to the strong correlation between the activation energy and conductivity prefactor, once one of the two parameters is known, the other is easily estimated (see discussion above and Figure 5a). These two parameters are the only values needed to calculate conductivity at any temperature using the Arrhenius or VFT equations. In effect, the activation energy fully describes the conductivity at any temperature. We therefore chose to remove these features from the statistical regression to avoid data leakage between the features and the target prediction value, the ionic conductivity. Highly correlated features (with correlation factors above 0.99) were also removed from the feature list to improve the interpretability of feature importances. Lastly, recursive feature elimination was used to optimize the total number of features used during learning, in an attempt to reduce the propensity for overfitting.

A random forest statistical regression analysis enables the extraction of electrolyte, monomer and anion features that are most important for calculating conductivity performance (Figure 6a). The electrolyte characteristics include the approximate molecular weight of the polymer, the approximate T_g of the electrolyte, the salt concentration, and whether the electrolyte is crystalline. The approximate T_g uses the T_g of the electrolyte, where provided, and otherwise substitutes the T_g of the pure polymer without salt added. Based on the discussion above, this is expected to be a good indicator of performance for some functional groups, while for others the trend was less clear. However, the pre-

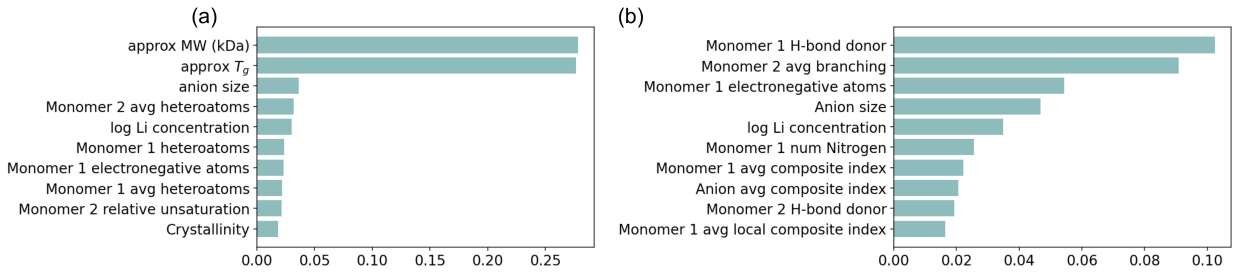

Figure 6: (a) Top ten electrolyte features extracted from trained random forest regressor including experimental features ranks approximate T_g and polymer approximate molecular weight highest, followed by salt concentration, monomer characteristics such as the presence of heteroatoms, and anion size. (b) Re-training the random forest regressor using a feature set without experimental parameters still indicates the importance of anion size, salt concentration, and monomer electronegative atoms, but also includes measures of monomer hydrogen bonding, as well as complexity including branching and composite indices.

vious analysis was using *only* T_g as a predictor, while in the regression models T_g is one of multiple features that is aggregated to predict performance. Equally important is the approximate molecular weight of the polymer electrolyte, which is the number-averaged molecular weight where provided, and otherwise the weight-averaged molecular weight. Previous studies have suggested molecular weight is an important factor for oligomeric systems, while it ceases to be important above a threshold value.[128] This was attributed to the link between polymer molecular weight and T_g at low molecular weights. In this dataset, it is likely that the approximate molecular weight feature is used as a composite proxy for a range of correlated features. While the approximate molecular weight shows only very weak correlation to other features included in the random forest model (see SI), it is likely more highly correlated with features that were previously eliminated in the recursive feature reduction. This is confirmed below when experimental features such as the molecular weight are eliminated from the random forest model, resulting in comparable performance.

Electrolyte salt concentration is also included in the top ten important features, suggesting that in conjunction with polymer T_g and molecular weight, it can play an important

role in conductivity performance. While the random forest feature importance does not provide information on the sign of the weighting of salt concentration, ridge regression can (see SI). Ridge regression suggests a small positive correlation between salt concentration and ionic conductivity. Many studies exploring the role of salt concentration at relatively low concentrations have shown that conductivity is nonmonotonic with salt concentration, reaching a maximum at intermediate salt concentration.[56,118] At higher salt concentrations (e.g. over 50 wt%), another improvement in conductivity seems to occur;[1] the sign of the coefficient for ridge regression possibly emphasizes the higher overall conductivities seen at very high salt concentrations.

Monomer features also contribute to the ionic conductivity performance, and include measures of the presence of electronegative and heteroatoms and of monomer complexity. Heteroatoms play an important role in salt dissociation, ion solvation and ionic conduction, and thus it is unsurprising that they dominate the monomer feature importance. However, the importance of heteroatom optimization for improved Li^+, rather than total, conductivity is not determined here because the performance metric observed in this study is total ionic conductivity.

For important anion characteristics, the measure of anion size (molecular bulk, 'alpha') plays the largest role and is the feature of third most importance, while oxygen atom count and number of hydrogen bonding acceptors are somewhat important but not ranked within the first ten features. Individual studies have shown that larger anions (e.g. $TFSI^-$) dissociate more readily and result in higher ionic conductivity compared to smaller anions (e.g. ClO_4^-);[129] while the general aggregate data does not show a strong trend in conductivity versus ion identity, statistical regression confirms anion size importance on conductivity performance.

A random forest regression procedure completed without the use of experimental features shows similar performance, suggesting that the uncertainty associated with measuring experimental parameters other than the ionic conductivity can be eliminated. The

new top ten most important features are shown in Figure 6b, while the similar training/validation scores are shown in the SI. While the mean validation errors do increase, the increase is rather small, implying that other electrolyte features provide reasonably identical predictive capability. This analysis points towards a simplified procedure for data extraction, as it suggests that experimental processing parameters and features such as the solvent and conditions used for polymer-salt mixing, molecular weight and polymer T_g are less important than is suggested by the initial regression analysis discussed above.

The most important parameters relating to ionic conductivity performance as extracted from statistical regression on this new feature set still focus on salt concentration, anion molecular bulk, and comonomer heteroatom count, confirming the importance of those parameters. The most important features also include a measure of the monomer branching coefficient, which can be seen as a proxy for monomer complexity or size, and may relate to the monomer free volume or the propensity for the polymer to crystallize.

Removing experimental features still enables adequate expected conductivity calculations for both the training and test datasets (see SI). The R^2, root mean squared error and mean absolute error are 0.71, 0.59 and 0.40, suggesting that on average the test data was predicted to be within 6 times the actual conductivity value. There are a few outliers within the data, but this error is within expected noise of conductivity measurements given the widely varying processing parameters and data quality that could not be accounted for in the data analysis due to lack of publication information.

Critically, the dataset and statistical regression models explored in this study cannot be used for novel polymer electrolyte performance prediction. Once the dataset splitting between train, validation and test is done by grouped polymer-anion entries, model performance drops precipitously (Figure 7). This splitting eliminates leakage of information between the training and validation or test sets, such as the generally similar performance of a single polymer-anion system. This underscores the inability of the models to predict polymer electrolyte performance for polymer-anion combinations that they have not pre-

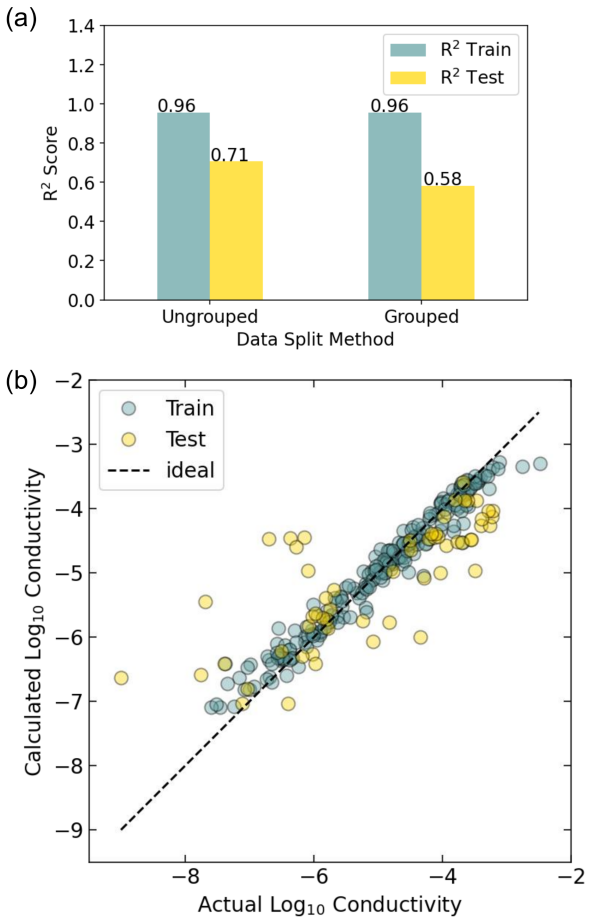

Figure 7: (a) Model performance on a test dataset with polymers not seen during training drops significantly compared to the ungrouped train-test split. (b) Actual versus predicted conductivity performance for the grouped random forest model reveals outliers for test dataset, emphasizing the failure of the model to accurately predict performance for new polymer chemistries.

viously seen during training. Recursive feature elimination in this case removes all but seven features to use for model training – these are approximate T_g, approximate molecular weight, the log10 of lithium to functional group ratio (salt concentration), comonomer 2 measure of heteroatoms ('eta F'), comonomer 2 molecular graph complexity ('eta RL'), comonomer 2 measure of electronegative atom count ('epsilon 1'), and anion number of hydrogen bond acceptors. The R^2 fit for the test dataset is 0.58 (and 0.37 for the five-fold cross-validation performance), indicating poor predictive capability. Thus, while the simple models examined here perform reasonably well at understanding and predicting performance when the polymer and anion identity is shared between the training and test sets, once the test set has significantly different characteristics compared to the training set, the models explored here struggle to recover predictive understanding. This suggests that perhaps the learnings obtained from a subset of polymer-anion combinations do not apply to other polymers or anions, and aligns well with the visualization results presented in Figure 4, where the T_g–conductivity trends of different polymer families can vary widely. The low performance of the models trained on grouped data emphasizes that such models should not be used to predict new polymer chemistries that are not related to those polymer-anion electrolyte combinations explored within the training data.

Conclusions

The curation and analysis of aggregated polymer electrolyte data from the literature provides insight both into the applicability of design rules across a large range of polymer classes, as well as into the difficulties and uncertainties associated with data quality and quantity. While studies on individual polymer families show correlations between T_g, anion size, and ionic conductivity, the aggregated data has much weaker trends in most features known or expected to control ion conduction. statistical learning on the aggregated data corroborates the importance of features such as T_g, monomer electronegative atom count,

and anion size. However, the models explored here are highly susceptible to overfitting, and show only small reductions in performance when experimental features such as T_g and processing conditions are left out. This suggests a highly correlated network of features from which no single feature dominates the landscape. While the ability to calculate conductivity performance without the need for additional experimental parameters opens opportunities for simplified data extraction and analysis in future conductivity datasets, these simple models can not be used for predictive purposes in cases where the polymer or anion is altered from those used in the training dataset, as was shown when constraining train-validation-test splittings to occur along polymer-anion groups. This emphasizes that the prediction and design of novel high performance polymer electrolytes is a challenging task that is not captured by the simple models or range of features explored in this study. Because of the relative lack of trends in existing databases, it is possible that other features such as processing metrics that are not commonly reported may be important in controlling ionic conductivity in these polymer systems. Future work in the field of polymer electrolytes must therefore focus on data quality and completeness.

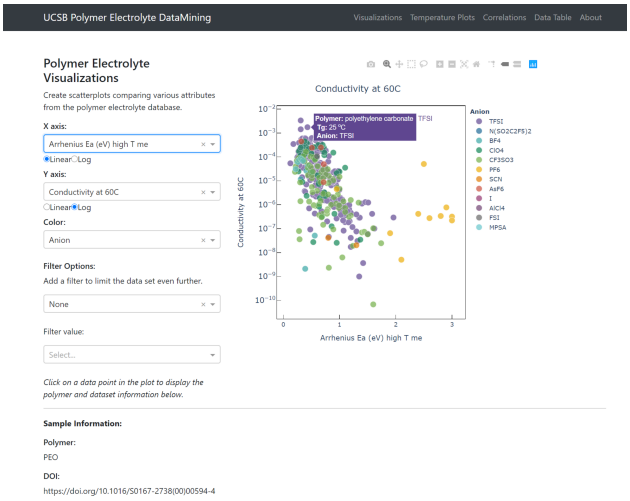

Figure 8: Screenshot of the interactive website created for interactive visualizations, temperature plotting, feature correlations, and access to the curated data spreadsheet and literature DOIs. The website can be found at `PEdatamine.org`.

The work included herein is not an exhaustive analysis of the curated data; the compi-

lation of an open-access polymer electrolyte database and web-based visualization enables interactive data analysis by other researchers for continued analysis and exploration (Figure 8, *https://PEdatamine.org*). The visualizations page allows a user to plot any two features against each other to explore possible trends and correlations. Further manipulation is available through color, as well as through specific filter drop-down menus that allow a user to limit the scope of the plotted data to a specific polymer family, publication DOI, salt identity, etc. The ability to explore trends from a specific feature in a sub-set of the extracted data aids in forming an understanding of possible correlations within a polymer family, etc., that might not translate across the entire spectrum of studied polymer electrolytes. Additional pages in the site allow a user to explore the raw conductivity data (with the ability to plot the data in Arrhenius, VFT, and temperature formats), feature correlations, and links to access the compiled data spreadsheets and original papers referenced in this study. We hope that such open-access web-based visualization will enable additional trends to be explored by other researchers in the field, further expanding the utility of the curated experimental database.

Acknowledgement

The authors would like to thank Steven Kauwe and Prof. Taylor Sparks for their early guidance on data curation and machine learning, and Kevin Wojcik for help with the website. This work was supported by the Materials Research Science and Engineering Program (MRSEC) of the National Science Foundation (NSF) under DMR 1720256 (IRG-2). N.S.S gratefully acknowledges the Fannie and John Hertz Foundation and the NSF Graduate Research Fellowship Program under DGE 1650114. Any opinions, findings, and conclusions or recommendations expressed in this material are those of the authors and do not necessarily reflect the views of the NSF.

Supporting Information

Link to GitHub for database information, additional visualization plots, statistical regression results for other regression models, feature correlations, calculated versus actual conductivity results.

References

(1) Mindemark, J.; Lacey, M. J.; Bowden, T.; Brandell, D. Beyond PEO - Alternative Host Materials for Li^+–Conducting Solid Polymer Electrolytes. *Prog. Polym. Sci.* **2018**, *81*, 114–143.

(2) Xue, Z.; He, D.; Xie, X. Poly(ethylene oxide)-Based Electrolytes for Lithium-Ion Batteries. *J. Mater. Chem. A* **2015**, *3*, 19218–19253.

(3) Schauser, N. S.; Seshadri, R.; Segalman, R. A. Multivalent Ion Conduction in Solid Polymer Systems. *Mol. Syst. Des. Eng.* **2019**, *4*, 263–279.

(4) Goodenough, J. B.; Kim, Y. Challenges for Rechargeable Li Batteries. *Chem. Mater.* **2010**, *22*, 587–603.

(5) Schauser, N. S.; Grzetic, D. J.; Tabassum, T.; Kliegle, G. A.; Le, M. L.; Susca, E. M.; Antoine, S.; Keller, T. J.; Delaney, K. T.; Han, S.; Seshadri, R.; Fredrickson, G. H.; Segalman, R. A. The Role of Backbone Polarity on Aggregation and Conduction of Ions in Polymer Electrolytes. *J. Am. Chem. Soc.* **2020**, *142*, 7055–7065.

(6) Pesko, D. M.; Jung, Y.; Hasan, A. L.; Webb, M. A.; Coates, G. W.; Miller III, T. F.; Balsara, N. P. Effect of Monomer Structure on Ionic Conductivity in a Systematic Set of Polyester Electrolytes. *Solid State Ionics* **2016**, *289*, 118–124.

(7) Tanaka, R.; Fujita, T.; Nishibayashi, H.; Saito, S. Ionic Conduction in Poly(ethylenimine)-and Poly(N-methylethylenimine)-Lithium Salt Systems. *Solid State Ionics* **1993**, *60*, 119–123.

(8) Sparks, T.; Gaultois, M.; Oliynyk, A.; Brgoch, J.; Meredig, B. Data Mining Our Way to the Next Generation of Thermoelectrics. *Scr. Mater.* **2016**, *111*, 10–15.

(9) Gaultois, M.; Oliynyk, A.; Mar, A.; Sparks, T.; Mulholland, G.; Meredig, B. Perspective: Web-based Machine Learning Models for Real-Time Screening of Thermoelectric Materials Properties. *APL Mater.* **2016**, *4*, 053213.

(10) Oliynyk, A.; Sparks, T.; Gaultois, M.; Ghadbeigi, L.; Mar, A. $Gd_{12}Co_{5.3}Bi$ and $Gd_{12}Co_5Bi$, Crystalline Doppelganger with Low Thermal Conductivities. *Inorg. Chem.* **2016**, *55*, 6625–6633.

(11) Sendek, A. D.; Yang, Q.; Cubuk, E. D.; Duerloo, K.-A. N.; Cui, Y.; Reed, E. J. Holistic Computational Structure Screening of More Than 12000 Candidates for Solid Lithium-Ion Conductor Materials. *Energy Environ. Sci.* **2017**, *10*, 306–320.

(12) Ahmad, Z.; Xie, T.; Maheshwari, C.; Grossman, J. C.; Viswanathan, V. Machine Learning Enabled Computational Screening of Inorganic Solid Electrolytes for Suppression of Dendrite Formation in Lithium Metal Anodes. *ACS Cent. Sci.* **2018**, *4*, 996–1006.

(13) Sendek, A. D.; Cubuk, E. D.; Antoniuk, E. R.; Cheon, G.; Cui, Y.; Reed, E. J. Machine Learning-Assisted Discovery of Solid Li-Ion Conducting Materials. *Chem. Mater.* **2019**, *31*, 342–352.

(14) Bobbitt, N. S.; Snurr, R. Q. Molecular Modelling and Machine Learning for High-Throughput Screening of Metal-Organic Frameworks for Hydrogen Storage. *Mol. Simul.* **2019**, *45*, 1069–1081.

(15) Gu, G. H.; Noh, J.; Kim, I.; Jung, Y. Machine Learning for Renewable Energy Materials. *J. Mater. Chem. A* **2019**, *7*, 17096–17117.

(16) Balachandran, P.; Kowalski, B.; Sehirlioglu, A.; Lookman, T. Experimental Search for High-Temperature Ferroelectric Perovskites Guided by Two-Step Machine Learning. *Nat. Commun.* **2018**, *9*, 1668.

(17) Zhuo, Y.; Mansouri Tehrani, A.; Brgoch, J. Predicting the Band Gaps of Inorganic Solids by Machine Learning. *J. Phys. Chem. Lett.* **2018**, *9*, 1668–1672.

(18) Zhuo, Y.; Tehrani, A.; Oliynyk, A.; Duke, A.; Brgoch, J. Identifying an Efficient, Thermally Robust Inorganic Phosphor Host via Machine Learning. *Nat. Commun.* **2018**, *9*, 4377.

(19) Cao, B.; Adutwum, L.; Oliynyk, A.; Luber, E.; Olsen, B.; Mar, A.; Buriak, J. How to Optimize Materials and Devices via Design of Experiments and Machine Learning: Demonstration Using Organic Photovoltaics. *ACS Nano* **2018**, *12*, 7434–7444.

(20) Kusne, A. G.; Gao, T.; Mehta, A.; Ke, L.; Nguyen, M. C.; Ho, K.-M.; Antropov, V.; Want, C.-Z.; Kramer, M. J.; Long, C.; Takeuchi, I. On-the-Fly Machine-Learning for High-Throughput Experiments: Search for Rare-Earth-Free Permanent Magnets. *Sci. Rep.* **2015**, *4*, 6367.

(21) Landrum, G.; Penzotti, J.; Putta, S. Machine-Learning Models for Combinatorial Catalyst Discovery. *Meas. Sci. Technol.* **2004**, *16*, 270–277.

(22) Jha, A.; Chandrasekaran, A.; Kim, C.; Ramprasad, R. Impact of Dataset Uncertainties on Machine Learning Model Predictions: the Example of Polymer Glass Transition Temperatures. *Model. Simul. Mater. Sci. Eng.* **2019**, *27*, 024002.

(23) Kim, C.; Chandrasekaran, A.; Jha, A.; Ramprasad, R. Active-Learning and Materials Design: The Example of High Glass Transition Temperature Polymers. *MRS Commun.* **2019**, *9*, 860–866.

(24) Yu, X. Support Vector Machine-Based QSPR for the Prediction of Glass Transition Temperatures of Polymers. *Fibers Polym.* **2010**, *11*, 757–766.

(25) Hatakeyama-Sato, K.; Tezuka, T.; Nishikitani, Y.; Nishide, H.; Oyaizu, K.; Hatakeyama-Sato, K.; Oyaizu, K. Synthesis of Lithium-ion Conducting Polymers De-

signed by Machine Learning-based Prediction and Screening. *Chem. Lett.* **2019**, *48*, 130–132.

(26) Hatakeyama-Sato, K.; Tezuka, T.; Umeki, M.; Oyaizu, K. AI-Assisted Exploration of Superionic Glass-Type Li^+ Conductors with Aromatic Structures. *J. Am. Chem. Soc.* **2020**, *142*, 3301–3305.

(27) Wang, Y.; Xie, T.; France-Lanord, A.; Berkley, A.; Johnson, J. A.; Shao-Horn, Y.; Grossman, J. C. Toward Designing Highly Conductive Polymer Electrolytes by Machine Learning Assisted Coarse-Grained Molecular Dynamics. *Chem. Mater.* **2020**, *32*, 4144–4151.

(28) Zhu, G.; Kim, C.; Chandrasekarn, A.; Everett, J. D.; Ramprasad, R.; Lively, R. P. Polymer Genome-Based Prediction of Gas Permeabilities in Polymers. *J. Polym. Eng.* **2020**, *40*, 451–457.

(29) Seshadri, R.; Sparks, T. D. Perspective: Interactive Material Property Databases Through Aggregation of Literature Data. *APL Mater.* **2016**, *4*, 053206.

(30) Ghadbeigi, L.; Harada, J. K.; Lettiere, B. R.; Sparks, T. D. Performance and Resource Considerations of Li-ion Battery Electrode Materials. *Energy Environ. Sci.* **2015**, *8*, 1640–1650.

(31) Gorai, P.; Gao, D.; Ortiz, B.; Miller, S.; Barnett, S. A.; Mason, T.; Lv, Q.; Stevanovic, V.; Toberer, E. S. TE Design Lab: A Virtual Laboratory for Thermoelectric Material Design. *Comput. Mater. Sci.* **2016**, *112*, 368–376.

(32) Wang, A. Y.-T.; Murdock, R. J.; Kauwe, S. K.; Oliynyk, A. O.; Gurlo, A.; Brgoch, J.; Persson, K. A.; Sparks, T. D. Machine Learning for Materials Scientists: An Introductory Guide toward Best Practices. *Chem. Mater.* **2020**, *31*, 4954–4965.

(33) Kauwe, S. K.; Rhone, T. D.; Sparks, T. D. Data-Driven Studies of Li-Ion-Battery Materials. *Crystals* **2019**, *9*, 54.

(34) Diederichsen, K. M.; Buss, H. G.; Mccloskey, B. D. The Compensation Effect in the Vogel-Tammann-Fulcher (VTF) Equation for Polymer-Based Electrolytes. *Macromolecules* **2017**, *50*, 3831–3840.

(35) Yelon, A.; Movaghar, B. Microscopic Explanation of the Compensation (Meyer-Neldel) Rule. *Phys. Rev. Lett.* **1990**, *65*, 618–620.

(36) Dyre, J. C. A Phenomenological Model for the Meyer-Neldel Rule. *J. Phys. C Solid State Phys.* **1986**, *19*, 5655–5664.

(37) Angulakshmi, N.; Nahm, K. S.; Nair, J. R.; Gerbaldi, C.; Bongiovanni, R.; Penazzi, N.; Stephan, A. M. Cycling Profile of $MgAl_2O_4$-Incorporated Composite Electrolytes Composed of PEO and $LiPF_6$ for Lithium Polymer Batteries. *Electrochim. Acta* **2013**, *90*, 179–185.

(38) Babu, H. V.; Srinivas, B.; Muralidharan, K. Design of Polymers with an Intrinsic Disordered Framework for Li-Ion Conducting Solid Polymer Electrolytes. *Polymer (Guildf)*. **2015**, *75*, 10–16.

(39) Ballard, D. G. H.; Cheshire, P.; Mann, T. S.; Przeworski, J. E. Ionic Conductivity in Organic Solids Derived from Amorphous Macromolecules. *Macromolecules* **1990**, *23*, 1256–1264.

(40) Bannister, D.; Davies, G.; Ward, I.; McIntyre, J. Ionic Conductivities of Poly(methoxy polyethylene glycol monomethacrylate) Complexes with $LiSO_3CH_3$. *Polymer (Guildf)*. **1984**, *25*, 1600–1602.

(41) Barteau, K. P.; Wolffs, M.; Lynd, N. A.; Fredrickson, G. H.; Kramer, E. J.;

Hawker, C. J. Allyl Glycidyl Ether-Based Polymer Electrolytes for Room Temperature Lithium Batteries. *Macromolecules* **2013**, *46*, 8988–8994.

(42) Buriez, O.; Han, Y. B.; Hou, J.; Kerr, J. B.; Qiao, J.; Sloop, S. E.; Tian, M.; Wang, S. Performance Limitations of Polymer Electrolytes Based on Ethylene Oxide Polymers. *J. Power Sources* **2000**, *89*, 149–155.

(43) Ek, G.; Jeschull, F.; Bowden, T.; Brandell, D. Li-Ion Batteries Using Electrolytes Based on Mixtures of Poly(vinyl alcohol) and Lithium bis(triflouromethane) sulfonamide Salt. *Electrochim. Acta* **2017**, *246*, 208–212.

(44) Erickson, M.; Frech, R.; Glatzhofer, D. T. Solid Polymer/Salt Electrolytes Based on Linear Poly((N-2-cyanoethyl)ethylenimine). *Electrochim. Acta* **2003**, *48*, 2059–2063.

(45) Fauteux, D.; Prud'Homme, J.; Harvey, P. E. Electrochemical Stability and Ionic Conductivity of Some Polymer-LiX Based Electrolytes. *Solid State Ionics* **1988**, *28-30*, 923–928.

(46) Ferry, A.; Edman, L.; Forsyth, M.; MacFarlane, D. R.; Sun, J. Connectivity, Ionic Interactions, and Migration in a Fast-Ion-Conducting Polymer-in-Salt Electrolyte Based on Poly(acrylonitrile) and $LiCF_3SO_3$. *J. Appl. Phys.* **1999**, *86*, 2346.

(47) Florjancyzk, Z.; Zygadło-Monikowska, E.; Wieczorek, W.; Ryszawy, A.; Tomaszewska, A.; Fredman, K.; Golodnitsky, D.; Peled, E.; Scrosati, B. Polymer-in-Salt Electrolytes Based on Acrylonitrile/Butyl Acrylate Copolymers and Lithium Salts. *J Phys Chem B* **2004**, *108*, 14907–14914.

(48) Florjanczyk, Z.; Zygadlo-Monikowska, E.; Raducha, D.; Such, K.; Wieczorek, W. Polymer Electrolytes Based on Sulfur Dioxide Copolymers. *Electrochim. Acta* **1992**, *37*, 1555–1558.

(49) Fonseca, C. P.; Rosa, D. S.; Gaboardi, F.; Neves, S. Development of a Biodegradable Polymer Electrolyte for Rechargeable Batteries. *J. Power Sources* **2006**, *155*, 381–384.

(50) Ibrahim, S.; Mohd Yassin, M.; Ahmad, R.; Rafie Johan, M. Effects of Various $LiPF_6$ Salt Concentrations on PEO-Based Solid Polymer Electrolytes. *Ionics (Kiel)*. **2011**, *17*, 399–405.

(51) Itoh, T.; Fujita, K.; Inoue, K.; Iwama, H.; Kondoh, K.; Uno, T.; Kubo, M. Solid Polymer Electrolytes Based on Alternating Copolymers of Vinyl Ethers with Methoxy Oligo(ethyleneoxy)ethyl Groups and Vinylene Carbonate. *Electrochim. Acta* **2013**, *112*, 221–229.

(52) Kalita, M.; Bukat, M.; Ciosek, M.; Siekierski, M.; Chung, S. H.; Rodríguez, T.; Greenbaum, S. G.; Kovarsky, R.; Golodnitsky, D.; Peled, E.; Zane, D.; Scrosati, B.; Wieczorek, W. Effect of Calixpyrrole in PEO-$LiBF_4$ Polymer Electrolytes. *Electrochim. Acta* **2005**, *50*, 3942–3948.

(53) Kaplan, M. L.; Rietman, E. A.; Cava, R. J. Crown Ether Enhancement of Ionic Conductivity in a Polymer-Salt System. *Solid State Ionics* **1987**, *25*, 37–40.

(54) Karmakar, A.; Ghosh, A. A Comparison of Ion Transport in Different Polyethylene Oxide-Lithium Salt Composite Electrolytes. *J. Appl. Phys* **2010**, *107*, 104113.

(55) Konieczynska, M. D.; Lin, X.; Zhang, H.; Grinstaff, M. W. Synthesis of Aliphatic Poly(ether 1,2-glycerol carbonate)s via Copolymerization of CO_2 with Glycidyl Ethers Using a Cobalt Salen Catalyst and Study of a Thermally Stable Solid Polymer Electrolyte. *ACS Macro Lett.* **2015**, *4*, 533–537.

(56) Lascaud, S.; Perrier, M.; Vallke, A.; Besner, S.; Prud'homme, J.; Armand, M. Phase Diagrams and Conductivity Behavior of Poly(ethylene oxide)-Molten Salt Rubbery Electrolytes. *Macromolecules* **1994**, *27*, 7469–7477.

(57) Lee, D. K.; Allcock, H. R. The Effects of Cations and Anions on the Ionic Conductivity of Poly[bis(2-(2-methoxyethoxy)ethoxy)phosphazene] Doped with Lithium and Magnesium Salts of Trifluoromethanesulfonate and Bis(trifluoromethanesulfonyl)imidate. *Solid State Ionics* **2010**, *181*, 1721–1726.

(58) Lee, Y.-C.; Ratner, M. A.; Shriver, D. F. Ionic Conductivity in the Poly(ethylene malonate) / Lithium Triflate System. *Solid State Ionics* **2001**, *138*, 273–276.

(59) Lin, C. K.; Wu, I. D. Investigating the Effect of Interaction Behavior on the Ionic Conductivity of Polyester/$LiClO_4$ Blend Systems. *Polymer (Guildf)*. **2011**, *52*, 4106–4113.

(60) Linden, E.; Owen, J. R. Conductivity Measurements on Amorphous PEO Copolymers. *Solid State Ionics* **1988**, *28-30*, 994–1000.

(61) MacFarlane, D. R.; Zhou, F.; Forsyth, M. Ion Conductivity in Amorphous Polymer/Salt Mixtures. *Solid State Ionics* **1998**, *113-115*, 193–197.

(62) Magistris, A.; Mustarelli, P.; Quartarone, E.; Tomasi, C. Transport and Thermal Properties of $(PEO)_n$-$LiPF_6$ Electrolytes for Super-Ambient Applications. *Solid State Ionics* **2000**, *136-137*, 1241–1247.

(63) Matsumoto, K.; Kakehashi, M.; Ouchi, H.; Yuasa, M.; Endo, T. Synthesis and Properties of Polycarbosilanes Having 5-Membered Cyclic Carbonate Groups as Solid Polymer Electrolytes. *Macromolecules* **2016**, *49*, 9441–9448.

(64) Mindemark, J.; Sun, B.; Brandell, D. High-Performance Solid Polymer Electrolytes for Lithium Batteries Operational at Ambient Temperature. *J. Power Sources* **2015**, *298*, 166–170.

(65) Mitsuda, H.; Uno, T.; Kubo, M.; Itoh, T. Solid Polymer Electrolytes Based on Poly(1,3-diacetyl-4-imidazolin-2-one). *Polym. Bull.* **2006**, *57*, 313–319.

(66) Motomatsu, J.; Kodama, H.; Furukawa, T.; Tominaga, Y. Dielectric Relaxation and Ionic Transport in Poly(ethylene carbonate)-based Electrolytes. *Polymers for Advanced Technologies* **2017**, *28*, 362–366.

(67) Munshi, M. A.; Owens, B. B. Ionic Transport in Poly(ethylene oxide) (PEO)-LiX Polymeric Solid Electrolyte. *Polym. J.* **1988**, *20*, 577–586.

(68) Nagaoka, K.; Naruse, H.; Shinohara, I.; Watanabe, M. High Ionic Conductivity in Poly(dimethyl siloxane-co-ethylene oxide) Dissolving Lithium Perchlorate. *J. Polym. Sci. Polym. Lett. Ed.* **1984**, *22*, 659–663.

(69) Nishimoto, A.; Watanabe, M.; Ikeda, Y.; Kohjiya, S. High Ionic Conductivity of new Polymer Electrolytes Based on High Molecular Weight Polyether Comb Polymers. *Electrochim. Acta* **1998**, *43*, 1177–1184.

(70) Okumura, T.; Nishimura, S. Lithium Ion Conductive Properties of Aliphatic Polycarbonate. *Solid State Ionics* **2014**, *267*, 68–73.

(71) Orädd, G.; Edman, L.; Ferry, A. Diffusion: A Comparison Between Liquid and Solid Polymer LiTFSI Electrolytes. *Solid State Ionics* **2002**, *152-153*, 131–136.

(72) Passiniemi, P.; Takkumaki, S.; Kankare, J.; Syrjama, M. Ionic Conduction in Ethylene Oxide-Propylene Oxide Copolymers Containing $LiClO_4$. *Solid State Ionics* **1988**, *28-30*, 1001–1003.

(73) Paul, J. L.; Jegat, C.; Lassègues, J. C. Branched Poly(ethyleneimine)-CF_3SO_3Li Complexes. *Electrochim. Acta* **1992**, *37*, 1623–1625.

(74) Pehlivan, I. B.; Marsal, R.; Niklasson, G. A.; Granqvist, C. G.; Georén, P. PEI-LiTFSI Electrolytes for Electrochromic Devices: Characterization by Differential Scanning Calorimetry and Viscosity Measurements. *Sol. Energy Mater. Sol. Cells* **2010**, *94*, 2399–2404.

(75) Pozyczka, K.; Marzantowicz, M.; Dygas, J. R.; Krok, F. Ionic Conductivity and Lithium Transference Number of Poly(ethylene oxide):LiTFSI System. *Electrochim. Acta* **2017**, *227*, 127–135.

(76) Przyłuski, J.; Wieczorek, W. Copolymer Electrolytes. *Solid State Ionics* **1992**, *53-56*, 1071–1076.

(77) Robitaille, C. D.; Fauteux, D. Phase Diagrams and Conductivity Characterization of Some PEO-LiX Electrolytes. *J. Electrochem. Soc* **1986**, *133*, 315–325.

(78) Sato, A.; Okumura, T.; Nishimura, S.; Yamamoto, H.; Ueyama, N. Lithium Ion Conductive Polymer Electrolyte by Side Group Rotation. *J. Power Sources.* **2005**; *146*, 23–426.

(79) Saunier, J.; Alloin, F.; Sanchez, J. Y. Electrochemical and Spectroscopic Studies of Polymethacrylonitrile Based Electrolytes. *Electrochim. Acta* **2000**, *45*, 1255–1263.

(80) Schauser, N. S.; Nikolaev, A.; Richardson, P. M.; Xie, S.; Johnson, K.; Susca, E. M.; Wang, H.; Seshadri, R.; Clement, R. J.; Read de Alaniz, J.; Segalman, R. A. The Glass Transition Temperature and Ion Binding Determine Conductivity and Lithium-Ion Transport in Polymer Electrolytes. *ACS Macro Lett.* **2020**, *10*, 104–109.

(81) Schauser, N. S.; Sanoja, G. E.; Bartels, J. M.; Jain, S. K.; Hu, J. G.; Han, S.; Walker, L. M.; Helgeson, M. E.; Seshadri, R.; Segalman, R. A. Decoupling Bulk Mechanics and Mono- and Multivalent Ion Transport in Polymers Based on Metal-Ligand Coordination. *Chem. Mater.* **2018**, *30*, 5759–5769.

(82) Jones, S. D.; Schauser, N. S.; Fredrickson, G. H.; Segalman, R. A. The Role of Polymer–Ion Interaction Strength on the Viscoelasticity and Conductivity of Solvent-Free Polymer Electrolytes. *Macromolecules* **2020**, *53*, 10574–10581.

(83) Sun, B.; Mindemark, J.; Edström, K.; Brandell, D. Polycarbonate-based Solid Polymer Electrolytes for Li-ion Batteries. *Solid State Ionics* **2014**, *262*, 738–742.

(84) Sun, B.; Mindemark, J.; Morozov, E. V.; Costa, L. T.; Bergman, M.; Johansson, P.; Fang, Y.; Furó, I.; Brandell, D. Ion Transport in Polycarbonate Based Solid Polymer Electrolytes: Experimental and Computational Investigations. *Phys. Chem. Chem. Phys* **2016**, *18*, 9504–9513.

(85) Sun, J.; Stone, G. M.; Balsara, N. P.; Zuckermann, R. N. Structure–Conductivity Relationship for Peptoid-Based PEO–Mimetic Polymer Electrolytes. *Macromolecules* **2012**, *45*, 5151–5156.

(86) Timachova, K.; Watanabe, H.; Balsara, N. P. Effect of Molecular Weight and Salt Concentration on Ion Transport and the Transference Number in Polymer Electrolytes. *Macromolecules* **2015**, *48*, 7882–7888.

(87) Tominaga, Y.; Nanthana, V.; Tohyama, D. Ionic Conduction in Poly(ethylene carbonate)-Based Rubbery Electrolytes Including Lithium Salts. *Polym. J.* **2012**, *44*, 1155–1158.

(88) Tominaga, Y.; Shimomura, T.; Nakamura, M. Alternating Copolymers of Carbon Dioxide with Glycidyl Ethers for Novel Ion-Conductive Polymer Electrolytes. *Polymer (Guildf).* **2010**, *51*, 4295–4298.

(89) Tominaga, Y.; Yamazaki, K.; Nanthana, V. Effect of Anions on Lithium Ion Conduction in Poly(ethylene carbonate)-based Polymer Electrolytes. *J. Electrochem. Soc.* **2015**, *162*, 3133–3136.

(90) Vallée, A.; Besner, S.; Prud'Homme, J. Comparative Study of Poly(ethylene oxide) Electrolytes Made with $LiN(CF_3SO_2)_2$, $LiCF_3SO_3$ and $LiClO_4$: Thermal Properties and Conductivity Behaviour. *Electrochim. Acta* **1992**, *37*, 1579–1583.

(91) Watanabe, M.; Endo, T.; Nishimoto, A.; Miura, K.; Yanagida, M. High Ionic Conductivity and Electrode Interface Properties of Polymer Electrolytes Based on High Molecular Weight Branched Polyether. *J. Power Sources* **1999**, *81-82*, 786–789.

(92) Watanabe, M.; Rikukawa, M.; Sanui, K.; Ogata, N. Effects of Polymer Structure and Incorporated Salt Species on Ionic Conductivity of Polymer Complexes Formed by Aliphatic Polyester and Alkali Metal Thiocyanate. *Macromolecules* **1986**, *19*, 188–192.

(93) Wei, X.; Shriver, D. F. Highly Conductive Polymer Electrolytes Containing Rigid Polymers. *Chem. Mater.* **1998**, *10*, 2307–2308.

(94) Xia, D. W.; Soltz, D.; Smid, J. Conductivities of Solid Polymer Electrolyte Complexes of Alkali Salts with Polymers of Methoxypolyethyleneglycol Methacrylates. *Solid State Ionics* **1984**, *14*, 221–224.

(95) Yoon, H.-K.; Chung, W.-S.; Jo, N.-J. Study on Ionic Transport Mechanism and Interactions Between Salt and Polymer Chain in PAN Based Solid Polymer Electrolytes Containing $LiCF_3SO_3$. *Electrochim. Acta* **2004**, *50*, 289–293.

(96) Zahurak, S. M.; Kaplan, M. L.; Murphy, D. W.; Cava, R. J. Phase Relationships and Conductivity of the Polymer Electrolytes Poly (ethylene oxide)/Lithium Tetrafluoroborate and Polyethylene oxide)/Lithium Trifluoromethanesulfonate. *Macromolecules* **1988**, *21*, 654–660.

(97) Zardalidis, G.; Ioannou, E.; Pispas, S.; Floudas, G. Relating Structure, Viscoelasticity, and Local Mobility to Conductivity in PEO/LiTf Electrolytes. *Macromolecules* **2013**, *46*, 2705–2714.

(98) Zhang, H.; Liu, C.; Zheng, L.; Xu, F.; Feng, W.; Li, H.; Huang, X.; Armand, M.; Nie, J.; Zhou, Z. Lithium Bis(fluorosulfonyl)imide/Poly(ethylene oxide) Polymer Electrolyte. *Electrochim. Acta* **2014**, *133*, 529–538.

(99) WebPlotDigitizer; Version 4.4: Rohatgi, A. Pacfica CA 2020. https://automeris.io/WebPlotDigitizer (accessed 2021-05-27).

(100) Moriwaki, H.; Tian, Y.-S.; Kawashita, N.; Takagi, T. Mordred: a Molecular Descriptor Calculator. *J. Cheminform.* **2018**, *10*, 4.

(101) Lin, T. S.; Coley, C. W.; Mochigase, H.; Beech, H. K.; Wang, W.; Wang, Z.; Woods, E.; Craig, S. L.; Johnson, J. A.; Kalow, J. A.; Jensen, K. F.; Olsen, B. D. BigSMILES: A Structurally-Based Line Notation for Describing Macromolecules. *ACS Cent. Sci.* **2019**, *5*, 1523–1531.

(102) Hunter, J. D. Matplotlib: A 2D Graphics Environment. *Comput. Sci. Eng.* **2007**, *9*, 90–95.

(103) Plotly: Collaborative Data Science; Plotly Technologies Inc.: Montréal, QC 2015; https://plot.ly (accessed 2021-05-27) .

(104) Pedregosa, F. et al. Scikit-learn Machine Learning in Python. *J. Mach. Learn. Res.* **2011**, *12*, 2825–2830.

(105) Fenton, D. E.; Parker, J. M.; Wright, P. V. Complexes of Alkali Metal Ions with Poly(ethylene Oxide). *Polymer* **1973**, *14*, 589.

(106) Mongcopa, K. S. I.; Tyagi, M.; Mailoa, J. P.; Samsonidze, G.; Kozinsky, B.; Mullin, S. A.; Gribble, D. A.; Watanabe, H.; Balsara, N. P. Relationship between Segmental Dynamics Measured by Quasi-Elastic Neutron Scattering and Conductivity in Polymer Electrolytes. *ACS Macro Lett.* **2018**, *7*, 504–508.

(107) Ganesan, V.; Pyramitsyn, V.; Bertoni, C.; Shah, M. Mechanisms Underlying Ion Transport in Lamellar Block Copolymer Membranes. *ACS Macro Lett.* **2012**, *1*, 513–518.

(108) Ratner, M. A.; Shriver, D. F. Ion Transport in Solvent-Free Polymers. *Chem. Rev.* **1988**, *88*, 109–124.

(109) Bocharova, V.; Sokolov, A. P. Perspectives for Polymer Electrolytes: A View from Fundamentals of Ionic Conductivity. *Macromolecules* **2020**, *53*, 4141–4157.

(110) Shah, D. B.; Olson, K. R.; Karny, A.; Mecham, S. J.; Desimone, J. M.; Balsara, N. P. Effect of Anion Size on Conductivity and Transference Number of Perfluoroether Electrolytes with Lithium Salts. *J. Electrochem. Soc.* **2017**, *164*, A3511–A3517.

(111) Blonsky, P. M.; Shriver, D. F.; Austin, P.; Allcock, H. R. Complex Formation and Ionic Conductivity of Polyphosphazene Solid Electrolytes. *Solid State Ionics* **1986**, *18*, 258–264.

(112) Wheatle, B. K.; Keith, J. R.; Mogurampelly, S.; Lynd, N. A.; Ganesan, V. Influence of Dielectric Constant on Ionic Transport in Polyether- Based Electrolytes. *ACS Macro Lett.* **2017**, *6*, 1362–1367.

(113) Wheatle, B. K.; Lynd, N. A.; Ganesan, V. Effect of Polymer Polarity on Ion Transport: A Competition between Ion Aggregation and Polymer Segmental Dynamics. *ACS Macro Lett.* **2018**, *7*, 1149–1154.

(114) Choi, U. H.; Ye, Y.; Salas De La Cruz, D.; Liu, W.; Winey, K. I.; Elabd, Y. A.; Runt, J.; Colby, R. H. Dielectric and Viscoelastic Responses of Imidazolium-Based Ionomers with Different Counterions and Side Chain Lengths. *Macromolecules* **2014**, *47*, 777–790.

(115) Barteau, K. P. Poly(Glycidyl Ether)-Based Battery Electrolytes: Correlating Polymer Properties to Ion Transport. Ph.D. thesis, University of California, Santa Barbara, 2015.

(116) Stacy, E. W.; Gainaru, C. P.; Gobet, M.; Wojnarowska, Z.; Bocharova, V.; Greenbaum, S. G.; Sokolov, A. P. Fundamental Limitations of Ionic Conductivity in Polymerized Ionic Liquids. *Macromolecules* **2018**, *51*, 8637–8645.

(117) Diederichsen, K. M.; Fong, K. D.; Terrell, R. C.; Persson, K. A.; McCloskey, B. D. Investigation of Solvent Type and Salt Addition in High Transference Number Nonaqueous Polyelectrolyte Solutions for Lithium Ion Batteries. *Macromolecules* **2018**, *51*, 8761–8771.

(118) Sanoja, G. E.; Schauser, N. S.; Bartels, J. M.; Evans, C. M.; Helgeson, M. E.; Seshadri, R.; Segalman, R. A. Ion Transport in Dynamic Polymer Networks Based on Metal–Ligand Coordination: Effect of Cross-Linker Concentration. *Macromolecules* **2018**, *51*, 2017–2026.

(119) Shukla, N.; Thakur, A. K. Role of Salt Concentration on Conductivity Optimization and Structural Phase Separation in a Solid Polymer Electrolyte Based on PMMA-$LiClO_4$. *Ionics (Kiel)*. **2009**, *15*, 357–367.

(120) Borodin, O.; Smith, G. D. Mechanism of Ion Transport in Amorphous Poly(ethylene oxide)/ LiTFSI from Molecular Dynamics Simulations. *Macromolecules* **2006**, *39*, 1620–1629.

(121) Wang, Y.; Fan, F.; Agapov, A. L.; Yu, X.; Hong, K.; Mays, J.; Sokolov, A. P. Design of Superionic Polymers - New Insights from Walden Plot Analysis. *Solid State Ionics* **2014**, *262*, 782–784.

(122) Druger, S. D.; Ratner, M. A.; Nitzan, A. Polymeric Solid Electrolytes: Dynamic Bond Percolation and Free Volume Models for Diffusion. *Solid State Ionics* **1983**, *9*, 1115–1120.

(123) Druger, S. D.; Nitzan, A.; Ratner, M. A. Dynamic Bond Percolation Theory: A Mi-

croscopic Model for Diffusion in Dynamically Disordered Systems. I. Definition and One-Dimensional Case. *J. Chem. Phys* **1983**, *79*, 3133–3142.

(124) Druger, S. D.; Ratner, M. A.; Nitzan, A. Generalized Hopping Model for Frequency-Dependent Transport in a Dynamically Disordered Medium, with Applications to Polymer Solid Electrolytes. *Phys. Rev. B* **1985**, *31*, 3939–3947.

(125) Nitzan, A.; Ratner, M. A. Conduction in Polymers: Dynamic Disorder Transport. *J. Phys. Chem* **1994**, *98*, 1765–1775.

(126) Wieczorek, W. Entropy Effects on Conductivity of the Blend-Based and Composite Polymer Solid Electrolytes. *Solid State Ionics* **1992**, *53-56*, 1064–1070.

(127) Freeman, B. D. Basis of Permeability/Selectivity Tradeoff Relations in Polymeric Gas Separation Membranes. *Macromolecules* **1999**, *32*, 375–380.

(128) Teran, A. A.; Tang, M. H.; Mullin, S. A.; Balsara, N. P. Effect of Molecular Weight on Conductivity of Polymer Electrolytes. *Solid State Ionics* **2011**, *203*, 18–21.

(129) Wang, S.; Jeung, S.; Min, K. The Effects of Anion Structure of Lithium Salts on the Properties of in-situ Polymerized Thermoplastic Polyurethane Electrolytes. *Polymer (Guildf)*. **2010**, *51*, 2864–2871.

Graphical TOC Entry

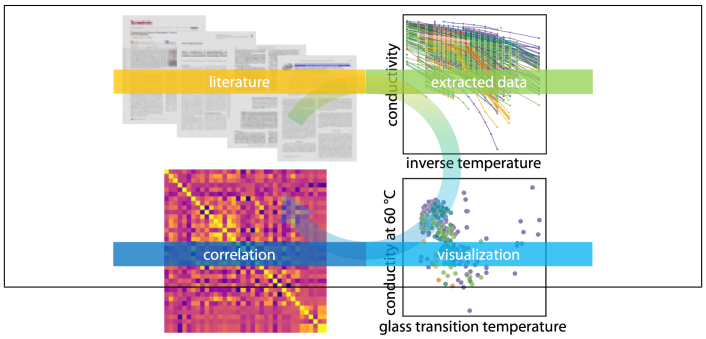

Supporting Information for: Database Creation, Visualization, and Statistical Learning for Polymer Li^+ Electrolyte Design

Nicole S. Schauser,[†,‡,¶] Gabrielle Kliegle,[§] Piper Cooke,[§] Rachel A. Segalman,[*,‡,†,‖] and Ram Seshadri[*,‡,†,§]

†*Materials Department*

University of California, Santa Barbara, Santa Barbara, California 93106, United States

‡*Materials Research Laboratory*

University of California, Santa Barbara, Santa Barbara, California 93106, United States

¶*Mitsubishi Chemical Center for Advanced Materials*

University of California, Santa Barbara, Santa Barbara, California 93106, United States

§*Department of Chemistry and Biochemistry*

University of California, Santa Barbara, Santa Barbara, California 93106, United States

‖*Department of Chemical Engineering*

University of California, Santa Barbara, Santa Barbara, California 93106, United States

E-mail: segalman@ucsb.edu; seshadri@mrl.ucsb.edu

Python scripts

All Python scripts and data files can be accessed at

`https://github.com/nschauser/PolymerElectrolyte`.

Data visualization website

All of the data presented in the work can be visualized on `https://PEdatamine.org`.

Data visualization

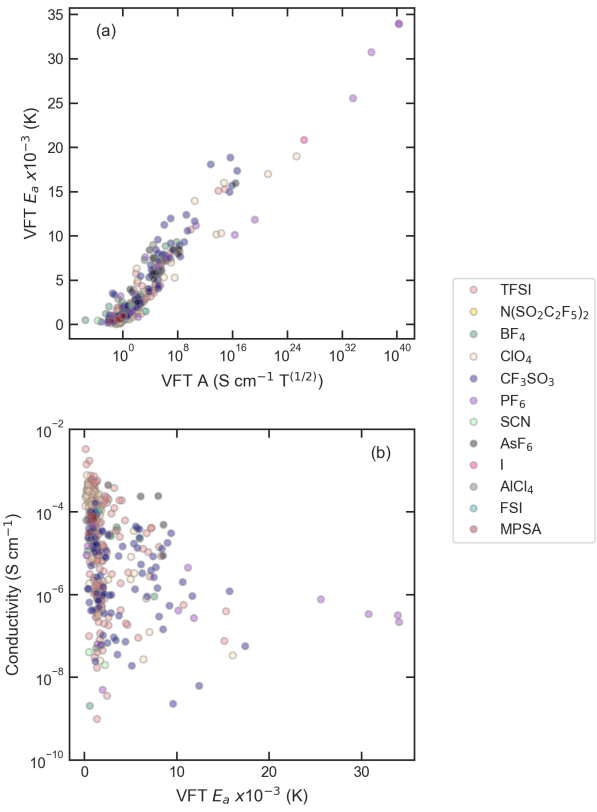

Figure S. 1: (a) VFT activation energy correlates with conductivity pre-factor, confirming the generality of the Meyer-Neldel rule. (b) VFT activation energy correlates somewhat with ionic conductivity, though more outliers and data spread exist compared to the Arrhenius E_a.

The activation energies extracted from conductivity-*vs*-temperature plots for the various collected data suggests a correlation between the Arrhenius activation energy and the conductivity, with a much weaker trend for VFT-based pseudo-activation energies (Figure 1b). Activation energy represents an estimate of the enthalpic contribution to the hopping barrier for ion mobility through the polymer matrix. Thus, it is perhaps unsurprising that a lower energy barrier for motion generally results in higher overall conductivity performance. What is surprising, is that the Arrhenius E_a provides a stronger correlation than the pseudo-activation energy obtained from VFT fits. Most polymer electrolyte performance extracted in this study was better represented in VFT format compared to Arrhenius. However, since the conductivity of most samples is measured over a relatively small temperature range, Arrhenius and VFT fits are generally not widely variant from each other, which could explain the relatively strong trend between Arrhenius activation energy and conductivity. Nevertheless, the VFT activation energy parameter exhibited a larger spread in values obtained through the fitting program, and does not provide as clear of a trend in conductivity performance. One possible explanation is the increase in fitting parameters for a full VFT equation, resulting in greater uncertainty of the obtained fit values. It is also possible that the more exact fit provided by the VFT equation captures experimental error inherent across the spread of publications, while the Arrhenius fitting essentially smoothes out uncertainty and error.

Statistical regression analysis

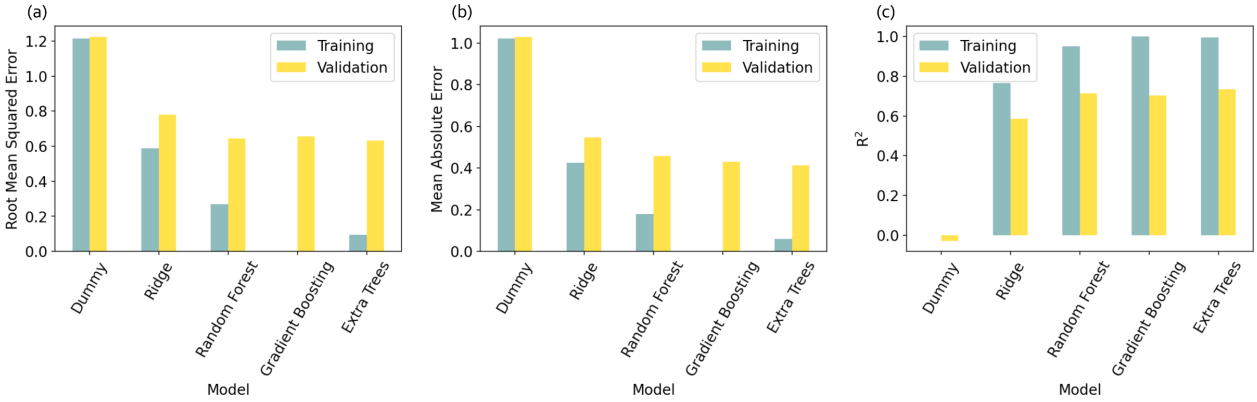

Figure S.2: Model performance in terms of (a) root mean square error, (b) mean absolute error and (c) R^2 for training and validation data during 5-fold cross-validation. Random forest model performance is best in all performance metrics.

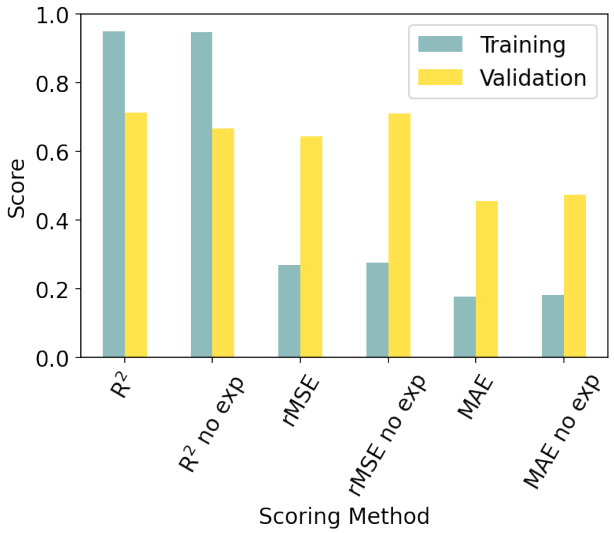

Figure S.3: Random forest regression models trained on feature set that includes experimental parameters compared to one without experimental parameters show similar performance.

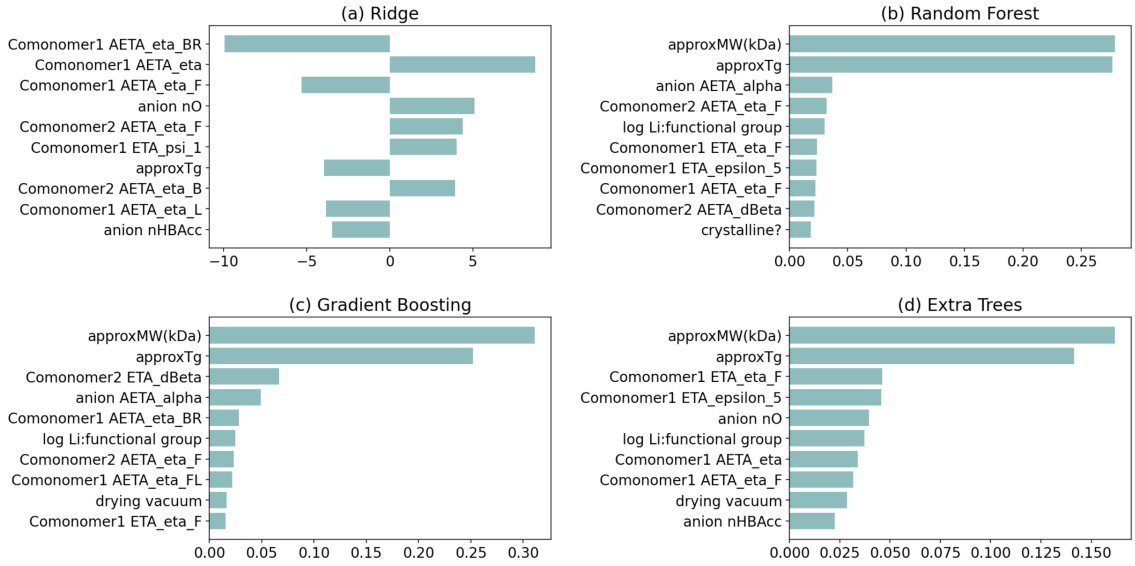

Figure S.4: Top ten most important features extracted from (a) Ridge regression, (b) Random Forest regression, (c) Gradient Boosting regression and (d) Extra Trees regression models trained on the training dataset using the 36 features including experimental parameters. (b) is the same as Figure 6b in the main text.

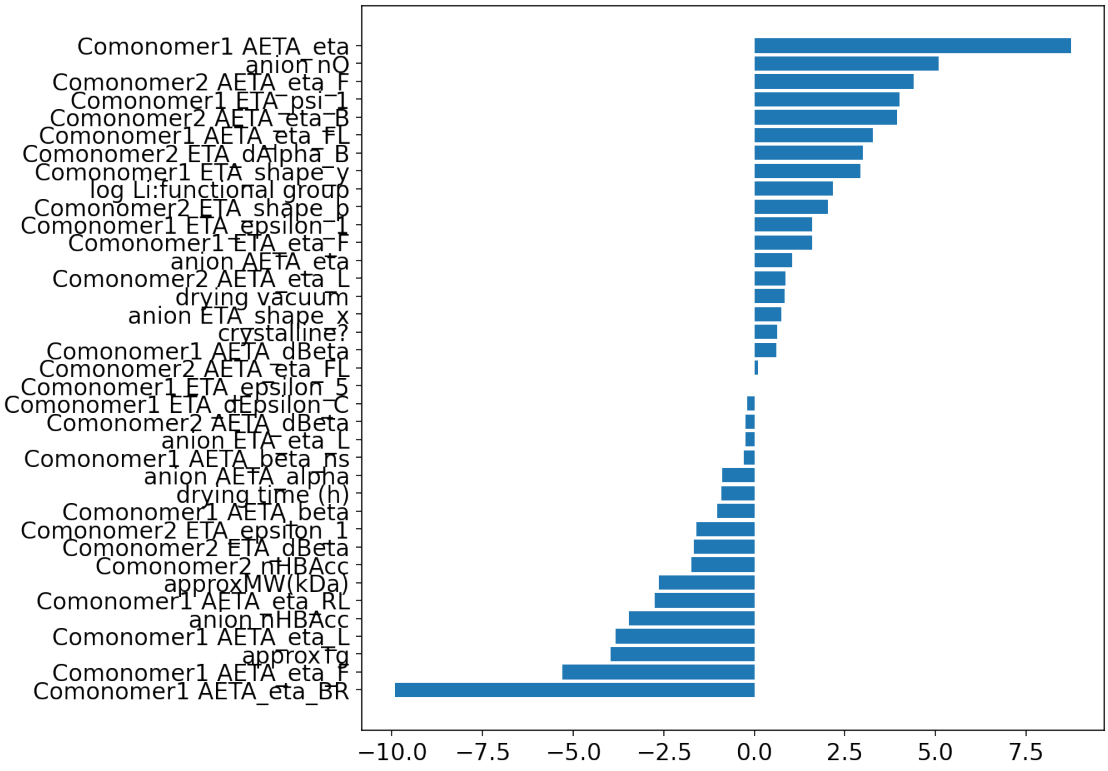

Figure S.5: Ordered feature importance for all 36 features for the ridge regression model, which shows both positive and negative correlations. Salt concentration (log Li:functional group) shows a positive correlation while T_g shows negative correlation.

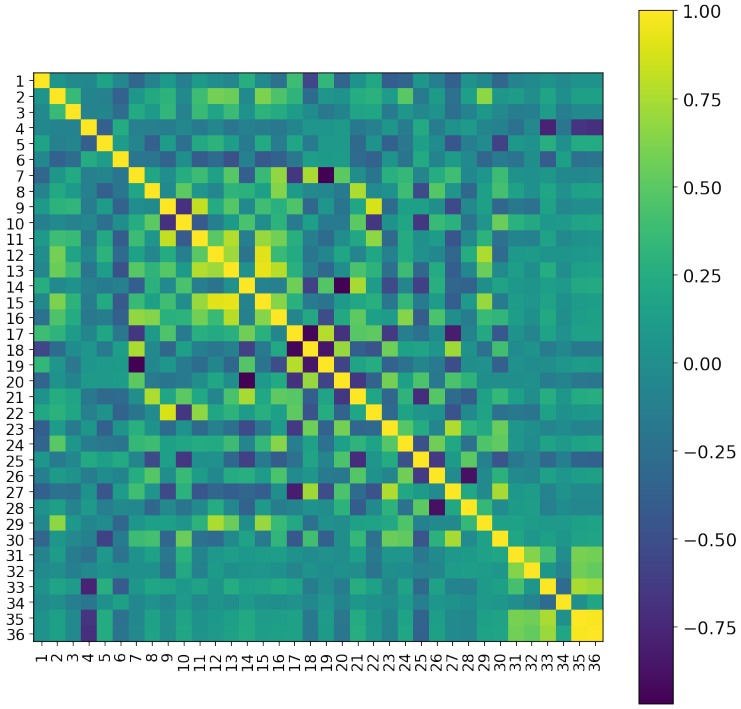

Figure S. 6: A correlation matrix of the 36 features used for statistical regression show generally weak correlations, though some monomer features are still correlated with each other, possibly slightly affecting feature importance rankings. The numbered features are described in Table 1

Table 1: Features chosen through recursive feature elimination for stastistical regression, numbered for easier reference in Figure 6.

Feature number	Feature	Descriptions
1	approximate MW (kDa)	
2	approximate T_g	
3	log Li:functional group	log molar salt concentration
4	drying time (h)	
5	drying vacuum	'high', 'regular', 'none'
6	crystalline?	is the electrolyte crystalline?: 'yes', 'no', 'n/a'
7	Comonomer1 ETA_epsilon_1	measure of electronegative atom count
8	Comonomer1 ETA_eta_F	functionality index - presence of heteroatoms
9	Comonomer1 AETA_eta_BR	averaged branching index, ring count
10	Comonomer1 AETA_eta_RL	averaged local reference alkane composite index
11	Comonomer1 ETA_shape_y	shape index describes size and shape of monomer
12	Comonomer1 AETA_dBeta	averaged measure of relative unsaturation content
13	Comonomer AETA_beta	averaged valence electron mobile count
14	Comonomer AETA_eta_L	averaged local composite index, bonded interactions
15	Comonomer1 AETA_beta_ns	averaged nonsigma contribution to valence electron mobile count
16	Comonomer1 AETA_eta_F	averaged functionality index - presence of heteratoms
17	Comonomer1 ETA_psi_1	hydrogen bonding propensity
18	Comonomer1 ETA_epsilon_5	measure of electronegative atom count
19	Comonomer1 ETA_dEpsilon_C	measure of electronegativity contribution
20	Comonomer AETA_eta_FL	averaged local functionality index - presence of heteroatoms
21	Comonomer1 AETA_eta	averaged measure of electronegativity
22	Comonomer2 AETA_eta_B	averaged branching index
23	Comonomer2 AETA_eta_FL	averaged local functionality index - presence of heteratoms
24	Comonomer2 AETA_eta_F	averaged functionality index - presence of heteratoms
25	Comonomer2 ETA_shape_p	shape index describes size and shape of monomer
26	Comonomer2 nHBAcc	number hydrogen bond acceptors
27	Comonomer2 ETA_dAlpha_B	count of hydrogen bond acceptor atoms/polar surface area
28	Comonomer2 ETA_dBeta	measure of relative unsaturation content
29	Comonomer2 AETA_dBeta	averaged measure of relative unsaturation content
30	Comonomer2 ETA_epsilon_1	measure of electronegative atom count
31	anion ETA_eta_L	local composite index, bonded interactions
32	anion AETA_eta	averaged measure of electronegativity
33	anion ETA_shape_x	shape index describes size and shape of monomer
34	anion AETA_alpha	average core count of a non-hydrogen vertex
35	anion nO	number of oxygen atoms
36	anion nHBAcc	number hydrogen bond acceptors

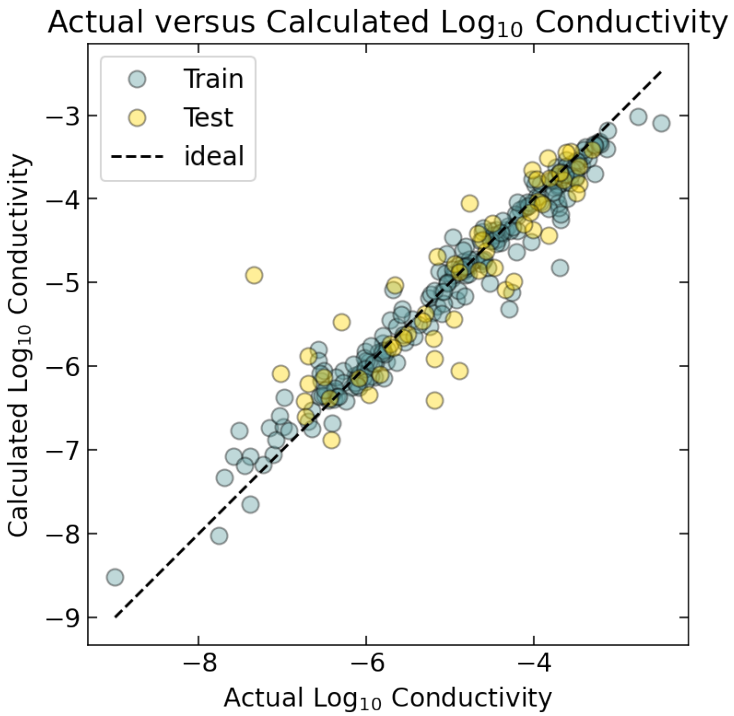

Figure S. 7: Random forest actual versus calculated conductivity performance at 60 °C when experimental features are included in the model. Similar to Figure S.8, where experimental features were removed for training.

Table 2: Cross-validated performance of all tested models when implementing polymer-anion grouped train-validation-test splitting.

Metric	Dummy	Ridge	Random Forest	Gradient Boosting	Extra Trees
Train					
Root Mean Squared Error	1.12	0.80	0.24	0.11	0.14
Mean Absolute Error	0.94	0.62	0.17	0.08	0.09
R^2	0	0.49	0.95	0.99	0.99
Validation					
Root Mean Squared Error	1.13	0.92	0.89	0.89	0.83
Mean Absolute Error	0.94	0.72	0.65	0.67	0.62
R^2	−0.02	0.32	0.37	0.36	0.44

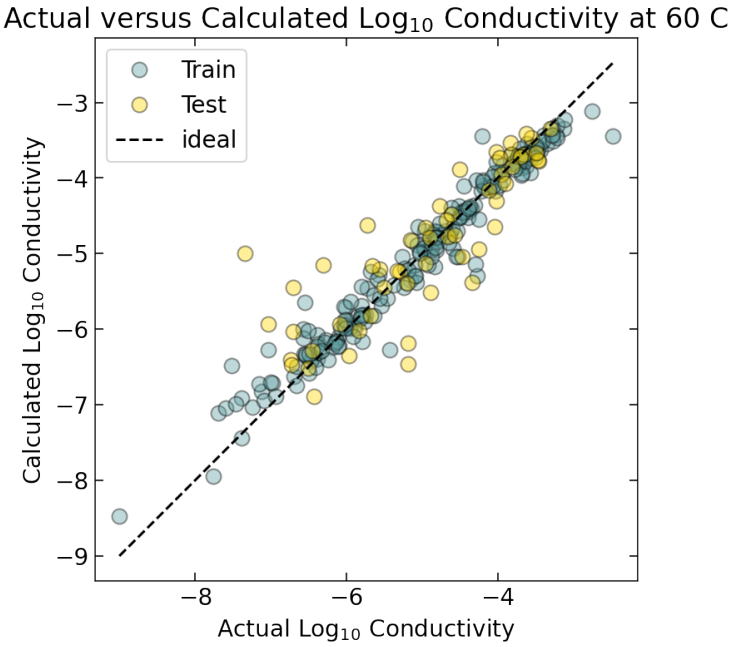

Figure S.8: Model performance for calculating conductivity on both the training and test datasets can be best visualized by plotting actual versus calculated conductivity for the optimized random forest regression model trained without experimental features. Most data falls within half an order of magnitude of the expected values, with a few outliers, especially for the test dataset.